STRUCTURAL DESIGN OF 3-AXIS CNC MACHINE TOOL FOR WOOD CARVING

A Dissertation Submitted

In Partial Fulfillment of the Requirements

for the Degree of

Master of Engineering

in

CAD/CAM Engineering

by

Sashank Thapa

801281020

to the

MECHANICAL ENGINEERING DEPARTMENT

THAPAR UNIVERSITY, PATIALA

July, 2014

CERTIFICATE

I hereby declare that the thesis entitled "**STRUCTURAL DESIGN OF 3-AXIS CNC MACHINE TOOL FOR WOOD CARVING** " is an authentic record of my study carried out as requirements for the award of the degree of **Master of Engineering** in **CAD/CAM Engineering** at **Thapar University, Patiala** under the supervision of **Mr. Sandeep Sharma, Assistant professor** ,Mechanical Engineering department, Thapar University, Patiala and Mr. **Ravinder Kumar Duvedi, Assistant professor,** Mechanical Engineering department, Thapar University, Patiala. During July, 2013 to July, 2014. The matter embodied in this report has not been submitted in partial or full to any other university or institute for the award of any degree.

Date: 15/07/2014

Sashank Thapa
ROLL NO: 801281020

It is certified that the above statement made by the student is correct to the best of my/our knowledge and belief.

Mr. Sandeep Sharma
Mechanical Engineering Department
Thapar University, Patiala - 147004

Mr. Ravinder Kumar Duvedi
Mechanical Engineering Department
Thapar University, Patiala - 147004

Countersigned by

Dr.Ajay Batish
Mechanical Engineering Department
Thapar University, Patiala - 147004

Dr. S.K.Mahopatra
Mechanical Engineering Department
Thapar University, Patiala - 147004

ACKNOWLEDGEMENT

I state my truthful gratitude to my guides Mr. Sandeep Sharma, Assistant Professor, Mechanical Engineering Department and Mr. Ravinder Kumar Duvedi, Assistant Professor, Mechanical Engineering Department, Thapar University, Patiala, for their valuable direction, proper advice and constant support during the course of my thesis work.

I do not find enough words with which I can express my feeling of thanks to the entire faculty and staff of Mechanical Engineering Department, Thapar University, for their help, inspiration and moral support which went a long way in successful completion of thesis work.

(SASHANK THAPA)

ABSTRACT

Wood carving from the ancient time is an attractive work for the decorative purposes and basic pattern demand. Earlier it was done by few skilled labors but from past decade due to increase in demand of items for decoration because of high life style is been done with the help of machine tools. The scenario is totally changed with the invent of CNC machines. As the close tolerance is needed for this purpose CNC machines are best suitable for this work because with the CNC machine this is achieved which add towards the beauty of the carving. In the present work an effort is made to design a wood carving CNC machine which will be optimized side by side while designing. As most of the company manufacturing the CNC wood carving machine does not disclose the procedure of designing so it is difficult to select a machine according to own input parameters. The work done here is having the initial step of study of numerical and empirical relationship required for the selection of various machine tool components followed by setting up the operating parameters which influences the machine tool selection. The standard components are selected against the designed components and the non standard components are selected such that can be easily manufactured. The Analysis of the machine tool components are done in ANSYS to check the deflection which can add towards the tool deflection the main cause for the tool path deviation. So optimization is done to minimize the deflection of machine tool components against its own self weight, cutting forces, long lengths of drives etc .In the present work knowledge of machine design, solid mechanics, strength of material and FEM software is used to do the whole work.

CONTENTS

LIST OF FIGURES

LIST OF TABLES

NOMENCLATURE

Symbol	Description
L_T	Length of tool
D	Diameter of tool
d	Depth of cut
f	Feed rate
Z	No. of teeth
f_Z	Feed per rotation
w	Width of cut
V_c	Cutting speed
N	Spindle rpm
$\mathrm{L_X}, \mathrm{L_Y}, \mathrm{L_Z}$	Length of X, Y and Z axis Traverse respectively
α	Maximum acceleration for X, Y and Z-axis drives
x	Nominal X-axis position
y	Nominal Y-axis position
z	Nominal Z-axis position
K_C	Maximum Specific cutting force considered for hardest wood
K	Maximum specific cutting power considered for hardest wood
Q	Material removal rate
P_f	Spindle power required
F_T	Tangential cutting force
K'	Geometry factor of the tip of the tool
T_P	Spindle torque required for plunging
P_P	Spindle power required for plunge milling
F_P	Thrust Force in plunge milling
F_m	Maximum cutting force out of face and plunge milling
P_S	Maximum spindle Power required for face or plunge milling
L_f	Loss factor
P_{max}	Maximum Spindle power required
$P_{standard}$	Nearest Standard spindle power available
m_s	Mass of standard spindle
σ_b	Bearing stress of selected Bracket material
B_t	Thickness of bracket plate
M_{bkt}	Mass of designed Bracket

W_{bkt}	Weight of the bracket
d_b	Diameter of clamping holes on bracket calculated from different cutting conditions
$\sigma_{bcalculated}$	Analytically calculated bearing stress from Bracket
m_{asm1}	Total mass of Spindle and Bracket together (sub assembly-1)
W_{asm1}	Total weight of Spindle and Bracket together (sub assembly-1)
W_i	Inertia load of spindle only in x-axis direction
W	Total load acting on each bolt of sub assembly-1
N_b	Number of bolt used to clamp spindle+bracket on Z-axis drive plate
W_{dt}	Direct Tensile load on each bolt
L_v	Vertical distance of bolts from twisting edge
L	Distance of the force vector from the twisting edge
w_b	Load on the bolt per unit distance
W_t	Tensile load on bolt
W_{mtb}	Maximum tensile load on group of bracket clamping bolts
σ_{bolt}	Tensile stress for bolt material
S_b	Factor of safety for clamp bolts
d_{bx}	Diameter of the bracket clamping bolt for cutting in x-axis
e_y	Eccentricity of the load when calculating bolt diameter for cutting in Y-axis
W_s	Direct shear load on each bolt
M_{ie}	Turning moment produced by the load W due to eccentricity e_y
L_c	Distance of bolt from centroid of sub assembly 1
S_{fb}	Secondary shear load on bolt
R_s	Resultant shear load on bolt
R_{smax}	Maximum Resultant Shear load on bolt
τ_{bolt}	Allowable shear stress for bolt material
d_{by}	Diameter of the bracket clamping bolt for cutting in Y-axis
W_P	Load on clamping bolts in plunge cutting
e_Z	Eccentricity of load in plunge cutting
W_{te}	Equivalent tensile Load
W_{se}	Equivalent shear Load
d_{btz}	Diameter of the bracket clamping bolt in tension in plunge cutting
d_{bsz}	Diameter of the bracket clamping bolt in shearing in plunge cutting

M_X, M_Y, M_Z Maximum bending moment in guide way in X, Y and Z axis direction respectively

l_{tx} Distance for force in X-axis cutting and point of moment in guide way

l_{ty} Distance for force in Y-axis cutting and point of moment in guide way

l_{pz} Distance for force in Z-axis cutting and point of moment in guide way

M_{Xa}, M_{Ya}, M_{Za} Allowable Maximum bending moment in guide way in X, Y and Z axis direction respectively

L_{fs} Distance out from ball screw that force is being applied

l_{bb} Center to center spacing of bearings

f_{bb} Resultant force on bearings by ball screw

$F_{\mu b}$ Friction force on each bearing

μ_b Coefficient of friction of round shaft

M_{Zback} Mass of the back plate of Z-axis of round shaft

M_{asm2} Mass of subassembly2 comprising of mass of subassembly 1 and back plate of Z

N_{mx}, N_{my}, N_{mz} Motor's rated rotational speed in X, Y and Z direction respectively

S_x, S_y, S_z Maximum Linear Speed of slide in X, Y and Z direction respectively

l_x, l_y, l_z Lead of screw in X, Y and Z slide respectively

t_{acc} Acceleration time

$\alpha_x, \alpha_y, \alpha_z$ Acceleration of slide in X, Y and Z direction respectively

$F_{fRx}, F_{fRy}, F_{fRz}$ Guide surface resistance in X, Y and Z slide respectively

F_{ax}, F_{ay}, F_{az} Axial load on ball screw in X, Y and Z direction respectively

η_{sc} Sliding screw efficiency

T_{tx}, T_{ty}, T_{tz} Driving torque to obtain thrust force in X, Y and Z direction respectively

d_{bsc} Diameter of ball screw according to maximum allowable stress

σ_{max} Maximum permissible von mises stress

d_{bav} Standard ball screw diameter available

L_{fx}, L_{fy}, L_{fz} Length of ball screw in X, Y and Z direction respectively

J_1 Mass moment of Inertia of pinion

J_2 Mass moment of Inertia of gear

J_3 Mass moment of Inertia of ball screw

J_4 Mass moment of Inertia of work and table

J_t Total Mass moment of Inertia

P_{rev} Pitch of ball screw in rev/mm

ρ	Density of ball screw material
N_b	Number of bolt used to clamp spindle+bracket on Z-axis drive plate
$r_{bx}, r_{by} r_{bz},$	Radius of ball screw rod in X, Y and Z direction respectively
μ	Co-effcient of friction of ball screw
e	Transmission efficiency of Ball screw
T_α	Acceleration torque
T_g	Gravity torque
T_f	Friction torque
T_{total}	Total torque
J_a	Mass moment of Inertia of driving side
J_l	Mass moment of Inertia of load side
J_K	Mass moment of Inertia of coupling
J_{motor}	Mass moment of Inertia of motor
J_{bs}	Mass moment of Inertia of ball screw
J_{sc}hl	Mass moment of Inertia of slide and work piece

Acronyms

ANSYS	Analysis System

Abbreviation

CNC	Computer numerical control
FEM	Finite element method
MCU	Machine control unit

CHAPTER: 1

INTRODUCTION

Wood working is one of the historic arts known to man that is being practiced from many centuries. In ancient era this was performed by hands using chisels and hammers which needed a tremendous amount of skill, labor and time. The birth of machine tools sparked the idea of automating this hard to master art so that wooden designs can be accurately created with less effort and in short span of time. Now days it is a fashion to have sculptured design in the doors of the big hotels and homes of rich peoples. Not only the doors but demand of all other decorative objects made of wood carving is increasing. Many small scale companies are there which offer various designs and very attractive costs. This is a result of revolutionized improvement and innovation in wood carving methods using computer controlled machines known as CNC routers. One such 3-axis router is designed using today's available modeling software and then this design is optimized for best performance and building cost. The procedure followed for this is discussed in forthcoming chapters of this thesis report.

1.1 EVALUATION OF WOOD CARVING

It is the propensity of human nature to embellish every possible article. Carving in wood is done with the help of tools, which results in a wooden sculpture, or in the beautification of a wooden object like wooden vases, doors etc. Primitive wood carving was performed by hands with the help of chisel or some pointed objects. The finished artifact's quality was totally contingent on the labor skills which was very hard to master and consumed a good amount of time. Wooden patterns are preferred over other materials as it is cheap and available in abundance, it can be easily shaped into different forms and intricate designs, its manipulation is easy because of lightness in weight, good surface finish can be easily obtained by only planning and sanding and it can be preserved for a fairly long time by applying proper preservatives like shellac varnish. Though wood cannot endure for a long time due to its tendency to absorb moisture and being eaten by insects still in some places all over the world sculptured wooden objects are found that are believed to be shaped thousands of year ago. There are reports of the North American Indian of carving there wooden fish-hook just as the Polynesian works patterns on his blade. The native of Guyana decorates with a well-conceived scheme of incised scrolls, while the inhabitant of Loango Bay carve there spoon with a design of perhaps figures standing up in full relief carrying a

Hammock [22]. In ancient effort to preserve the wooden figures for long time, they were painted using colors. W o r k were made to perform the wood carving work mechanically using machines, but not until the end of the eighteenth century. It was then any positive and practical ideas were described. Sir Samuel Bentham, an Englishman, patented in 1791 and 1793 principles of wood working which are in use even today. His inventions included "planning machines with rotary cutters to cut on several sides of the wood at once veneer cutting machines, moulding and recessing machines, bevel sawing machines, saw sharpening machine, tenon cutting machine by means of circular saws, boring tools"[23]. Though there are numerous tools available for wood working, either manually driven or electrically driven, but they need skillful hands to wield them. Development in field of computers made it possible the invention of computer controlled wood carving machines also known as routers which made wood carving process fast, more precise and crafting skills independent. Though these machines are capable of taking wood carving to sky high level but they still need human to guide them and command them to let miracles happen.

The more one recognizes the individualities of wood, the better one can appreciate the degree of warmth and beauty that it brings to our lifestyle. As each grain pattern in all type of woods is a unique chef-d'oeuvre of design, texture and majesty, people all over the world that owns goods made of wood can be assured that they are the only one in the world who owns that specific grain pattern and its natural beauty. Even flaws like knots or other natural blemishes can add more beauty and character to any given piece of wooden artifact. The density of a wood represents its mechanical properties. With change in species of source density of wood also changes. The taxonomy of wood has factually always been in terms of hard wood and soft wood. The hardwood for example wood from oak, maple,walnut are classified under dicotyledons and softwood for example pine and balsam arev classified under Conifers.

1.2.CNC ROUTER

A CNC router abbreviated as computer numeric control does carving with the help of machine tools. CNC router is improved form of hand held routers. CNC router are mounted on a device which guides the router through specified tool path. The tool travels on the confined path and used to cut a variety of materials varying from hardest to softest. A CNC router works similar to a CNC milling machine yet it differs from it in application of working material and so require tools that are significantly different in detail. The chip formation for both tools are different I terms of their mechanism, according to the materials. Routing is applied to wood, plastics and Aluminum, as these materialare weak in small sections, routers may be run at extremely high speeds and so even a small router may cut rapidly. The wood

router typically spins faster with a range of 13,000 to 24,000 RPM. A wood router is controlled with software specifically designed for use of wood routers.

Figure 1.1: Wood router [24]

As routing in different from a conventional milling process so design and thereafter material selection for the machine will be different.

1.2.1 Challenges for design of CNC wood router

(i) The router should spin above 15,000 RPM, instead of the 3,000 RPM, in order to cut wood instead of burning it. Due to which the following things should be considered

(ii) Tool be properly held and balanced. “Lack of stability in the tool generates vibration, which shortens tool life”.

(iii) To minimize vibration and resonance at high speeds.

(iv) Wood cutting machine process is characterized by multi axes high acceleration and deceleration phases and requires relevant electric energy amount to operate. This can cause electrical rack failure due to over-temperature operations, which decreases the efficiency of all the wood cutting process.

(v) The types of chips produced are in the form of dust which can produce jamming of machine components and environmental hazards.

(vi) As precision is the first demand from a wood router, so while making the machine precisely cost should be consider as a factor.

1.2.2 Types of commercial CNC routers

The CNC router are generally classified under number of axis. The axis of CNC router increase with the complexity of the work to be performed.

(i) 2-axis CNC router

These are low-end routers that are used by hobbyists for basic domestic items. These types of CNC routers do not have a true Z axis due to which they are not prominent for industrial

applications. These routers can produce figures on flat plate of constant depth. Example of such work is shown in figure 1.2.

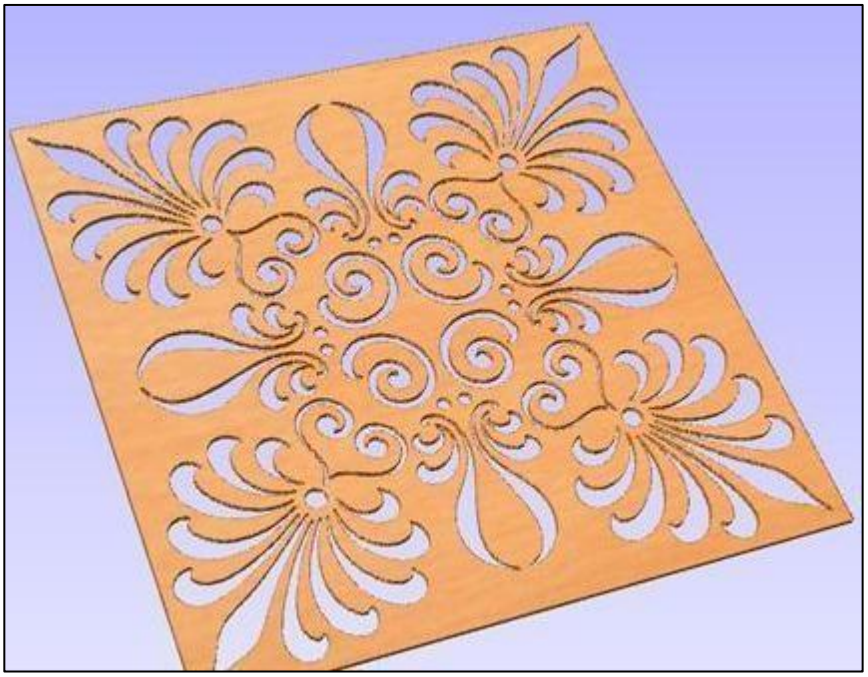

Figure 1.2: Example of wood Carving by 2-axis CNC router [25]

(ii) 3-axis CNC router

The 3 axis CNC router is the most commonly used CNC router as it can move tool in 3 directions i.e. X, Y and Z direction. Z direction is always along the length of the tool. Using this router carving perpendicular to surface of flat wooden plank can be done. Figure 1.1 shows a typical 3-axis CNC router and figure 1.3 shows an example of what these machines are capable of performing.

Figure 1.3: Example of wood Carving by 3-axis CNC router [26]

(iii) Turn mill CNC router

Turn mill are the machine tools having both the capability of rotate the tool as well as to rotate the work piece. Figure 1.4 shows a mill turn CNC router performing the turning as well as milling operation.

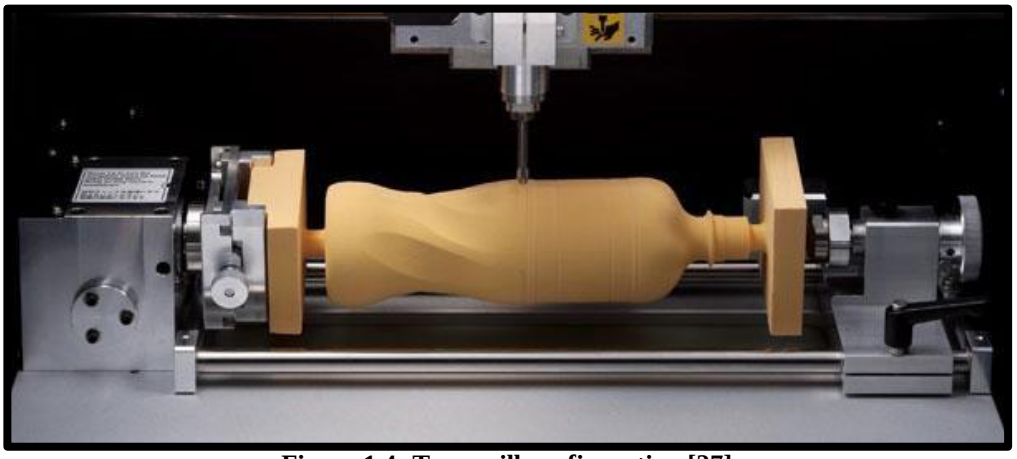

Figure 1.4: Turn mill configuration [27]

Figure 1.5: 5-axis CNC routers [28]

(iv) 5-axis CNC router

To cut the three dimensional object without moving the work pieces mainly used in Automobile, boat and aerospace 5-axis CNC routers are used which is having additional 2 axis apart from the basic three axis of the machine.

1.3 MAIN COMPONENTS OF A CNC ROUTER SYSTEM

CNC is a control system that receives a set of programmed directives, processes it and generates corresponding output control signals that control the motion of machine tool. It also process the feedback signals generated by various sensors and feedback devices mounted on the machine tool to ensure the proper execution of the directions given to the machine and

take appropriate actions if there is some error in execution of output commands. Figure 1.6 shows the schematics of a typical CNC machine.

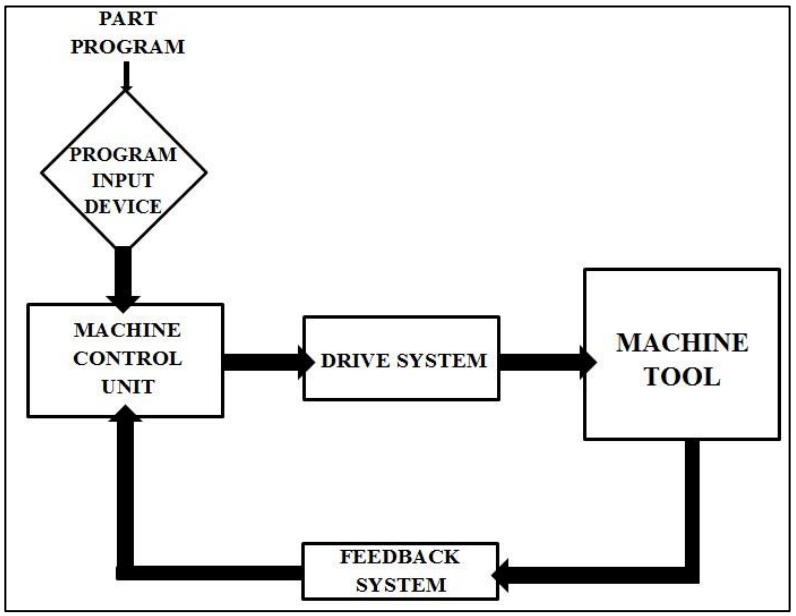

Figure 1.6: Schema of CNC machine

Major components of CNC includes part program, program input device, machine control unit, drive system, machine tool feedback system.

1.3.1 Part program

A part program is a set of instructions coded in terms of numbers, alphabets and symbols which are required to move the cutting tool in desired motion so that the required produce a part. It includes the instructions essential to control the movement of the machine tool and switch on/off the auxiliary functions of CNC machine such as spindle rotation and coolant.

1.3.2 Program input device

The part program are entered in the machine tool with the help of punched tapes/tape reader and build-in keyboard with the help of computers using RS-232-C cable interface. USB flash drives are also being used in latest form

1.3.3 Machine Control Unit

The machine control unit (MCU) can be referred as brain of a CNC machine. As functionality of our body is controlled by our brain in similar way it is MCU that controls the CNC machine. It performs following functions:

- Read the coded instructions through program input device.
- Decode the read instructions into small fragments line by line.
- Interpolate linear, circular and curved paths and generate motion commands for different axis.

- Transfers the generated motion commands to the amplifying circuits which in turn execute motion through drive system.
- Receives the feedback signals of position, speed and various other sensors and compensated the upcoming motion commands accordingly.
- Control auxiliary functions such as coolant on/off, spindle on/off and its rotation direction, tool change etc.

The important component of the MCU is the feedback system. The feedback system comprises of measuring devices and sensors that can estimate the state and condition of the CNC machine at any instant. For example encoders are used to determine the linear or angular position of the machine at any given instant. When a command or instruction is executed on the machine feedback system measures the output of the machine. This information is then fed to the MCU where it is compared to the reference values and as a result correction signals are generated for compensation in case if there is any error.

1.3.4 Drive System

Amplifier circuits drive motors, and ball lead-screws together constitutes drive system. The function of drive system is to execute motion commands as instructed by MCU. The MCU feeds the motion commands (i.e. position and speed) of every axis to the amplifier circuits. The command signals are amplified and are then fed to drive motors which in turn rotate the ball lead-screws to position the tool at the desired position.

1.3.5 Machine Tool

Machine tool is the body of the CNC machine. It is an assembly of constrained kinematic mechanism that is used to position the tool on the work piece and to move it relatively such that it can cause machining. It consists of various components like ball screws, guide ways, router/ spindle, machine bed, etc. The present work revolves around the selection of appropriate key components out of standard components available in market and to design the machine tool for wood carving.

1.4 KEY COMPONENT SELECTION AND DESIGN

The key component selection is the function of the factors such as cost minimization, work to be performed, availability of the material, precision and accuracy level. The recognition of the component required is an important step in designing and making any machine. After it has been recognized the necessary components the selection for the proper material and its designing should be done. The process will follow:

- The identification of working condition.
- Calculation of the forces.

- Calculation for the dimensions.

1.4.1 Ball screw

The ball screw is an mechanical component consisting of an assembly that changes rotating motion of motor to linear motion of drive and vice versa. The ball screw assembly consists of a ball screw and ball nut with Re-circulating ball bearings inside. The linking between the screw and the nut is made by ball bearings that revolve in the matching forms in the screw and ball nut. The forces transferred over a great number of ball bearings, giving a comparatively low relative load per ball. Due to rolling ball bearings the ball screw Drive has a very less friction coefficient. Ball Screw drives typically provide mechanical efficiency of greater than
90% so their higher initial cost is compensated by less power requirements. Ball screws are often preloaded. Preload serves following main purposes:

- It removes axial play between a screw shaft and a ball nut (i.e. Zero backlash).
- It reduces elastic deformation caused by outside force (i.e. Enhances rigidity).

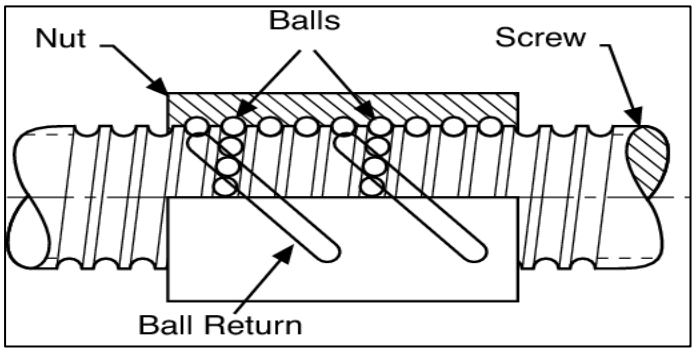

Figure 1.7: Cut section of a ball screw nut [29]

1.4.2 Guide ways

To ensure that the machine tool components moves in its predetermined track Guide ways are used which along with moving the machine tool along the correct path reduces the friction of motion . Factors to be consider for slide selection:

(i) Length of stroke and size
(ii) Mounting orientation.
(iii) Load to be carried out.
(iv) Maximum velocity.
(v) Acceleration and deceleration rate.
(vi) Service life.
(vii) Environment of work

Broadly two types of guide ways are available as discussed below.

(a) Linear motion guide ways

A linear motion guide way guides the motion of machine tool components smoothly which is derived with the help of ball screw. They drives the motion in all the three direction with prescribed accuracy and confined motion. Co-efficient of friction f linear motion guide way is 0.02 as compared to traditional slide

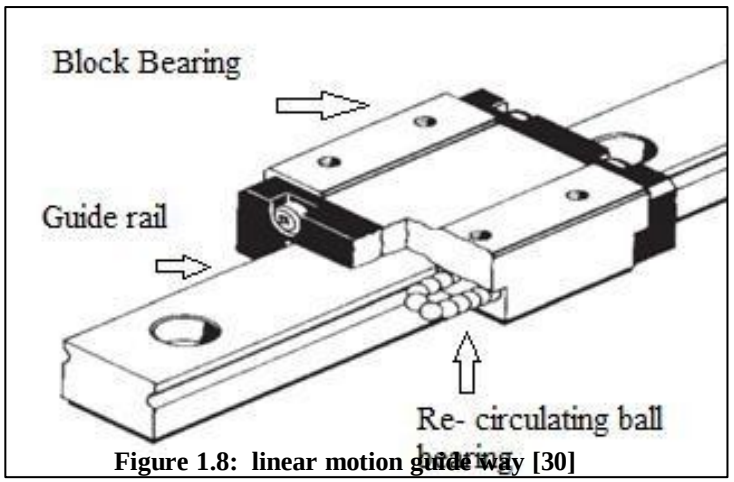

Figure 1.8: linear motion guide way [30]

The LM guide way mainly comprises of block bearing and guide rail. The Block bearing is composed of re circulated ball bearings which provides smooth motion over the guide rails

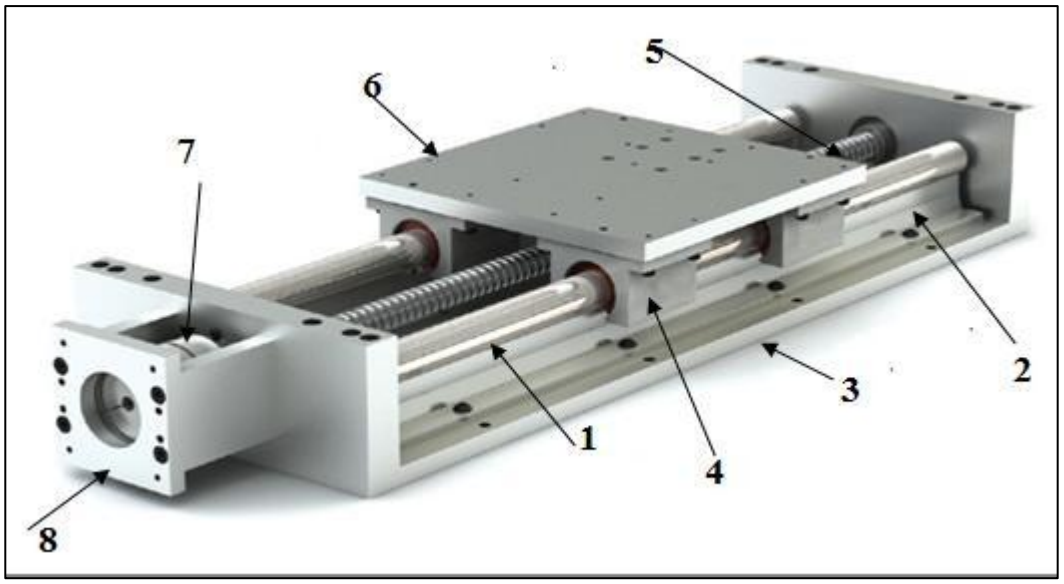

Figure 1.9: standard round shaft technology based machine drive system with plain bearing [31]

(b) Round shaft guide ways

Round shaft guide ways are used for working in dusty environment without any risk of chip inclusion. The round shaft ways use the ball screw assembly to transmit the rotary motion from drive motor to linear sliding motion of the slider mounted over the block bearings, whereas the block bearings are mounted over the round shafts. The figure 1.9 shows the various component of the standard round shaft technology based machine drive system, which are namely:

1. Circular solid steel rod
2. Aluminum alloy support for round shaft
3. Frame for supporting two round shaft supports
4. Block bearings
5. Ball screw assembly
6. Slider plate
7. Coupling (for transmitting rotary motion from motor to ball screw)
8. Motor housing (build in the frame)

The three main components of the round shaft guide ways comprising of round shaft, bearing and supporting rail has been shown in figure 1.10 with the markings a 1, 2 and 3 respectively.

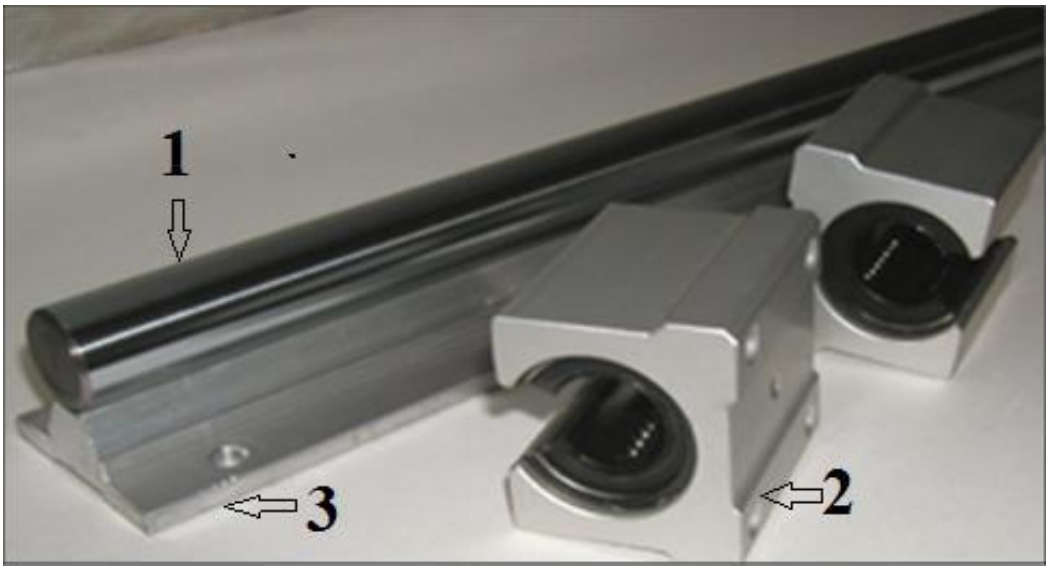

Figure 1.10: Main components of round shaft guide way [31]

The bearings are the most important part of the round shaft technology based machine drive system which helps transmit the motion in linear direction by minimizing the friction. Generally three types of bearings can be used with the round shaft technology based machine drive units as given below:

1. Bearing with recirculating ball
2. Bearing with preloaded non-recirculating balls
3. Plain Bearing

The recirculating and non-recalculated balls bearings are not suited for working in dusty environment like wood carving. Out of the above mentioned types the plain bearings have many advantages over linear ball bearing. These can be used in dirt, vibration, shock loading, welding, and foundry and wash down situations. These are made up of special liner material called Frelon, which is bonded to the bearing shaft which transfers the load and dissipates heat generated in the shaft. Frelon is a combination of Polytetrafluoroethylene (PTFE) with

some filler materials. PTFE is fiber material having self lubricating properties mainly used in making non-stick house hold utensils and has good vibration damping properties. Whereas filler material of has high load capacity, low wear rate and high strength are used in plain bearings. One such example of plain bearing is shown in figure 1.10. The plain bearings do not need any lubrication and when lubricated can work up to very high speed. Backlash is not a problem with them therefore they are not preloaded so have a longer life.

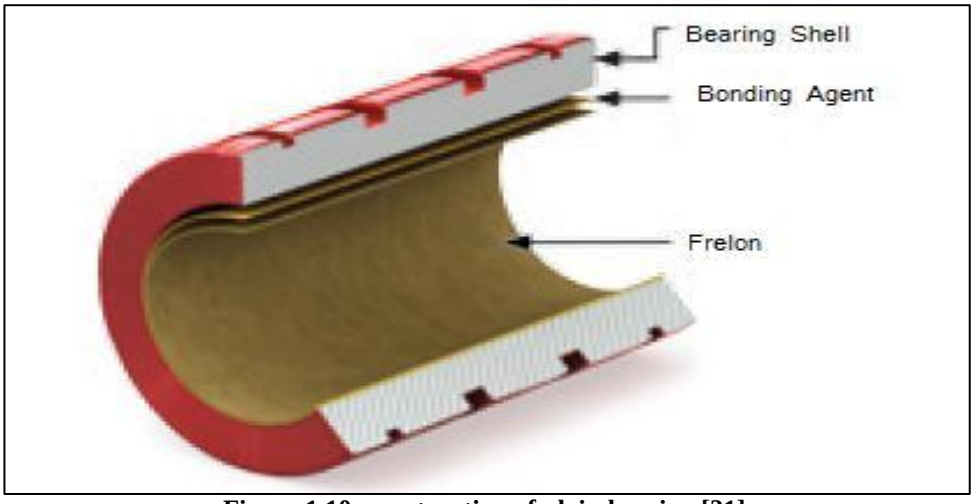

Figure 1.10: construction of plain bearing [31]

The round shaft guide ways are preferred over the LM guide ways for the work of wood carving because of the reason as compared in the table 1.1 below.

Table 1.1: Comparison of plain and ball bearing [14]

Bearing type	**Load**	**Moment load**	**Linear speed**	**Coefficient of friction**	**Precision**	**Environment**
Plain bearing	Up to 20 times of ball bearing	Limited to 2:1 ratio	1.524 m/sec in dry run 4.19 m/sec in lubrication.	0.125	Precision running clearance of 0.0127 mm per side	Excels in dry, contaminated, wet and clean room applications
Ball bearing	Limited due to point to point contact with shaft	Moderate to good	Up to 3 m/sec always required lubrication	0.05	Can be preloaded. This shortens life	Will fail and corrode in contaminated conditions

The conclusion from the comparision between plain and ball bearing types as given above has been used as guidline to select the round shaft instead of linear guideways.

The selection for the key dimensions of round shaft drive system for the presnt work is done on the basis of *permissible bending moment* for Z-axis and Y-axis motion. While for X-axis the selection depends upon the load carrying capacity required by the drive.

1.4.3 Router Motor

The router is a motor attached with a shaft having facility to hold interchangeable bits. A wood carving router is used for intermittent work and generally rotates at high Rpm than the machine motors. They are classified under type of cooling required and operation to be performed. A plunge router is preferred for the wood carving machine.

Figure 1.12: Wood carving router [32]

(i) Types of Router Motor

a) Fixed base router

b) The laminated Trimmer

c) Rotary tool router

d) Plunge router

A fixed base router as the name suggests is having a fixed base on which a motor is mounted with maximum power up to 0.5 horse power and tool shank diameter up to 0.5 inch. Whereas a laminated trimmer has a smaller capacity motor than fixed base and tool diameter up to 0.25 inch used to carve thin and narrow work pieces. They come in interchangeable bases. For more accurate and precise work on thin sections the rotary tool router were used having tool shank diameter up to 0.0625 inch. Now a day plunge router is used which performs all the carving work performed a router with the extra operation of plunging.

(ii) Cooling methods for router spindle

Router spindle of now a day performs the work of a machine tool spindle as well as motor rotor; therefore heat generation is major problem in this router spindle. In earlier times the spindle were driven with the help of gears and belt drives so at that time it was not a problem. As the router spindle is always in direct contact with work piece so proper care on heat dissipation methods should be considered. Air cooled and water cooled spindle are used for these purposes. Air cooled spindle is preferred while working with the wood carving operations to avoid moisture on the wood.

(iii) Power Rating

Power requirement for the router increases with the diameter of the tool and amount and level of carving which depends upon the depth and width of cut. For an wood carving operation the variety of wood varies from very soft wood to very hard wood but up to 5 kW power motor should be sufficient for this purpose.

(iv) Range of Speed

Speed of router motor is generally increases with the diameter of tool, with tool diameters less than one inch the speed can go up to 30,000 rpm. With more speed at large diameter of tool can burn the wood.

1.4.4 Bed for CNC wood router

Bed is among the critical component of the machine tool upon which all the weight and dynamic cutting force are acting. The bed should act as a vibration damping system but at the same time the weight of the bed should not increase to keep it with permissible cost and overall weight of the machine tool. The structural design of the bed earlier to its optimization in software is the work of a good engineer. Figure 1.13 shows the FEM analysis of a Bed done in ANSYS.

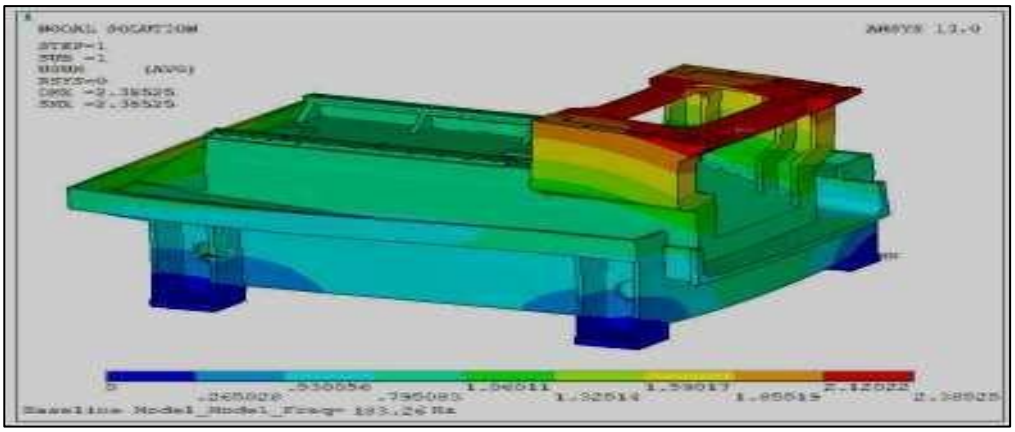

Figure 1.13: Fem modal analysis of optimization of bed [12]

1.4.5 Column

The columns can be loaded by force acting only in the plane of symmetry, e.g. drilling machine or by forces acting arbitrarily in space (e.g. vertical lathe, milling and boring machine, etc). The principal design requirement of column is the same as those of beds, i.e., high static and dynamic stiffness. These properties are achieved, as in the case of beds, by proper selection of the column material and its cross-section.

In general, machine tool column experiences:

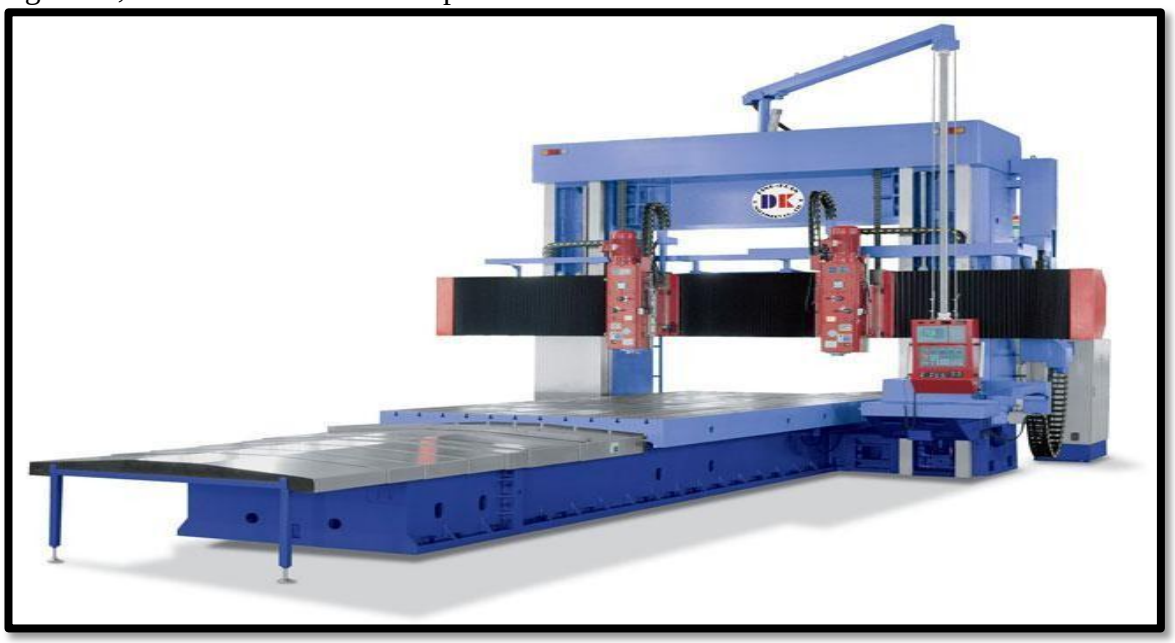

Figure 1.14: double column CNC router [33]

- Bending in two perpendicular planes,
- Shearing in two perpendicular planes, and
- Torsion.

1.4.6 Protection against wood dust

The fine wood dust can jam the drive system by blocking the ball screw groves or even it can enter in the motor causing its inefficient working. Apart from the wood dust there are some kind of fine stones found in the wood which grows with them creating serious problems.

Figure 1.15: wood dust on ball screw

Figure1.16: A dust collection vacuum pump installed in machine [34]

Dust in the form of wood chips which are very minute can cause serious health hazards and can jam the system. Therefore proper measures should be taken to remove dust. Dust generation while machining wood is caused by these factors:

- Standard chip thickness
- Moisture percentage of the wood
- feed direction and cutting angle

1.5. PRESENT WORK

The present work is to design a 3-axis CNC wood carving machine. The work table of the machine is to be designed to accommodate the largest standard wooden board sizes available in the Indian market, which is typically 6 feet by 8 feet (1828x2438 mm^2) in dimension. The machine design approach has been divided into two parts namely: selection of standard machine components available off the shelf in the market based on the required properties, and to design the non-standard structural support elements of the machine to hold the other key parts of machine in place within permissible deflection like gantry structure for holding Y-axis drive elements as shown in figure 1.17. The required span of work table needs the longer sizes of the support elements. Thus to design such a machine tool the main task is to keep the deflection of the machine drives minimum by designing the light weight as well as rigid structural elements.

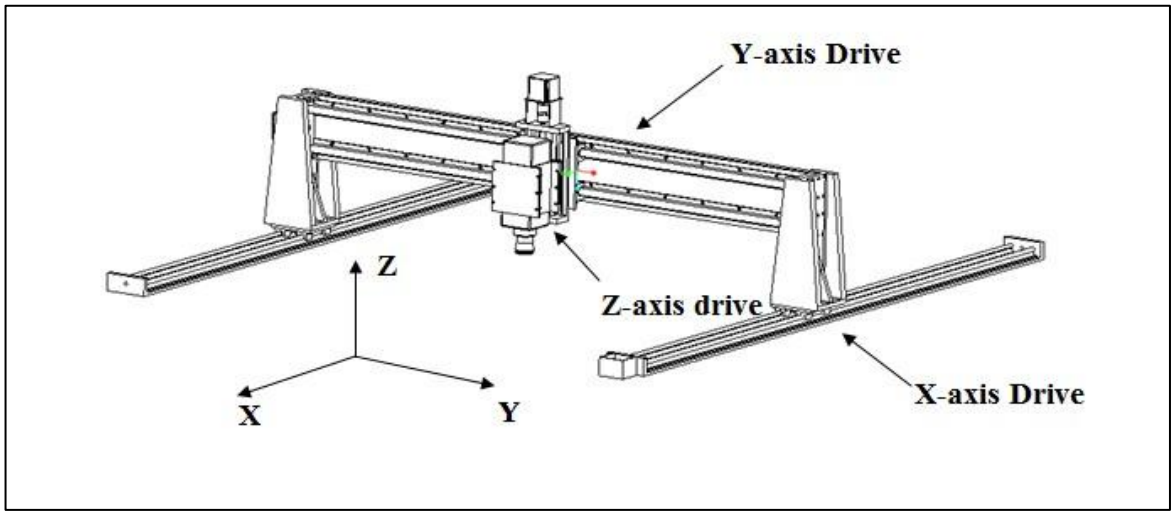

Figure1.17: Proposed model of wood carving machine structure.

One of the previously created designs of the wood carving machine [35] as shown in the figure 1.18 has been taken as a reference to model and redesign the machine tool in the present study.

The methodology for machine design used in the present work is based on a empirical relationship model presented in chapter 3, which is used to identify the magnitude of cutting

forces and kinds of loadings different machine elements will have to withstand based upon the initial given inputs like cutter shape and size to be used, properties of wood to be machined and machining conditions like speed, feed and maximum depth of cut. The value of required parameters from the empirical model has been used to find the standard part models and then the part model shapes from the given CAD dimensions from the selected vendor references has been used to create a valid 3D CAD model the parts in ProE environment. These part shapes has been further used to create the appropriate support elements part shapes like bracket for mounting spindle motor. These support elements along with the standard part model dimensions and material properties has been analyzed using ANSYS software for their deflection and stress conditions. The results of the FEM analysis for main parts have been presented in chapter 4. Further the conclusion of the study has been presented along with future scope in chapter 5.

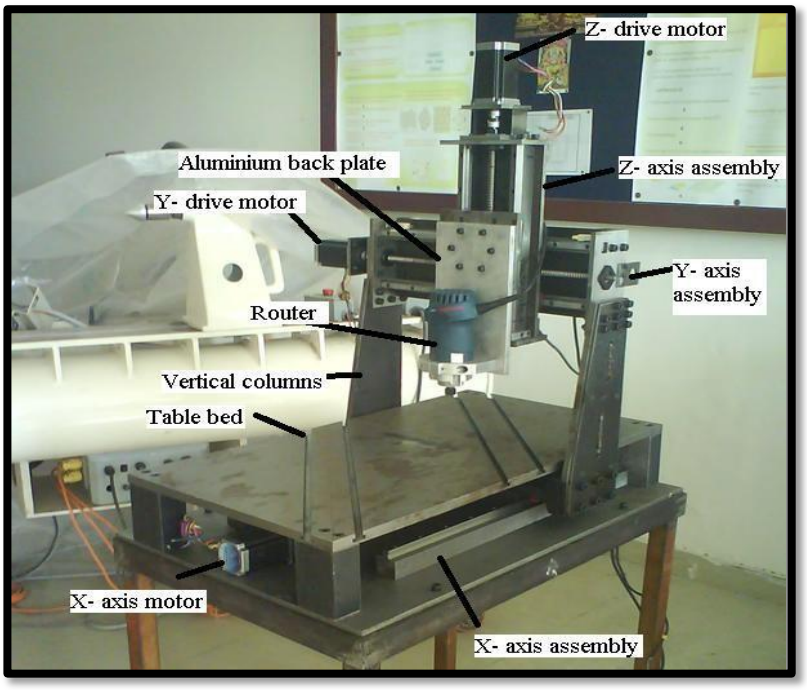

Figure1.18: 3-axis wood carving machine structure. [35]

CHAPTER: 2
LITERATURE REVIEW

The literature survey presented here is of the topic wise coverage of the different Components and the feature of the CNC wood cutting/carving router. Information collected from the research paper were used to proceed ahead towards the project and found to be very helpful. The literature surveyed has been divided into the different sections and presented below

2.1 MACHINING PROPERTIES OF WOOD

Holmberg et al. [1] write that like other cellular solids wood is a highly anisotropic material exhibiting a nonlinear stress-strain Behavior. The material property data depends upon the species and growth condition. They suggested the micro-macro modeling approach to find out the realistic material description. In this method FEM modeling of the wood structure is done on different layers of the wood.

Kopac and Sali [2] emphasized that increase in moisture content in wood structure enhances its machining property by decrease in cutting resistance but too much moisture content cause the tearing out of the fiber. The growth ring is composed of different layer of tissue density, the tool with circular motion when passes through these two alternative regions increases amplitude of vibration resulting in poor surface finish.

Malkocoglu[3] carried out test to study Machining properties and surface roughness of various wood species grown in different conditions. Effects of the rake angle and the feed speed were observed. The relationship between rake angle and surface roughness was surface were less smooth with increase in rake angle.

Rawangwong et al. [4] carried out the machining work on coconut wood; the result they find out was that the surface roughness changes with the feed rate. The result also shows that keeping the feed rate low and with higher cutting speed surface roughness reduces.

Boucher et al. [5] studied behavior of cutting force on different wood based material using the cutting tool helical in shape. Tooth is discretized further in order to form three orthogonal infinitesimal cutting forces from cutting constants. The methodology presented in this paper

can be improved in order to predict cutting forces for several materials and solid wood machining

Carmeli et al. [6] Wood cutting machine process is characterized by multi axes high acceleration and deceleration phases and requires relevant electric energy amount to operate. This can cause electrical rack failure due to over-temperature operations, which decreases the efficiency of all the wood cutting process. The present paper proposes an energy recovery system which can be adopted and installed also on existing machines and which allows to store the amount of energy produced during deceleration phases and to use this energy during the acceleration phases of the machine axis.

.

2.2 MACHINE STABILITY AND OPTIMIZATION.

suri et al. [7] consider tool deflection as the major component for the inaccuracy in the machine tool working, because of which it deviates from the original path given in the program. They have proposed the Cantilever beam method for the calculation of the tool deflection in FEM analysis.

yang and Choi [8] experimented that tool deflection is the major problem in achieving precision machining. They have work on the tool compensation methods in with after calculation of cutting force the surface error is find out and the tool position is adjusted with these techniques the error by tool deflection is reduced from 80 micron to 20 micron.

Zaeh and Oertli [9] studied that the Fem model of ball screw does not give satisfactory result because of flowing of two forces from it i.e. Torsional and axial force. They proposed the procedure for modeling and analysis of ball screw feed drive system which contains the making of stiffness matrix of all balls in contact with Nut and removing it with the spring elements.

Sobolewski[10] proposes that resonance frequency of driving system should not be equal to impact force in order to save the drive system from damage. .

Kono et al. [11] suggested the contact stiffness model for the optimization of bed design in which the contact stiffness is calculated from the unit stiffness of each support and floor which is multiplied by real contact area. This value of contact stiffness is than compared with the vibration modal shape and natural frequency obtained experimentally for its verification.

Lia et al. [12] proposed a procedure which is practical and simple for the design of machine tool bed. Complete design steps and effectiveness of the designed model is being studied in the paper

Zaehl et al. [13] Performed work for dynamic analysis of machine tool against the vibration in different machine structures and frames. A discrete geometric mapping method is used for modeling of components as finite element meshes, which are further combined to form machine tool models with the help of spring elements.

Jo¨nsson et al. [14] highlighted that in designing of CNC machine tools the static, dynamics and electrical components should be considered of machine tool at same time. The fully automated implementation system developed in this work is a capable base for dealing with this trade-off between productivity and accuracy of the production process through multidisciplinary optimization

2.3 FEED DRIVE

Fujita et al. [15] studied the working of linear guide way for improved accuracy and precision at high speed against the effect of table speed, global position and micro position experimentally.

Paweł Majda [16] studied the geometric errors to calculate joint kinematic errors in linear guide way with both experimentally and analytically. He found that these geometric errors leads to deformation and hence alter the kinematics of the system

Altintas et al. [17] concluded that continuous demand from the industry is a challenge for research to design such a spindle system rotating at high velocity and high feed rate simultaneously especially in case of micro machining. The physically experimentation by making prototype is found to very costly and time consuming and computational methods is preferred over it by mathematical representation.

Verl et al. [18] experimentally calculated the change in value of pretension in ball screw with the feed velocity. This result is helpful for the determination of life and efficiency of ball screw against preloading to avoid backlash.

2.4. CUTTING FORCE

Gradisek et al. [19] suggested a model for specific cutting force calculation in material which is always a constant value and differ from material to material named as Mechanistic force model. The factors of inputs are friction coefficient, work piece shear stress and shear angle and procedure of basic oblique cutting is applied.

Merdol et al. [20] gives a strategy for calculation of machining variables analytically and experimentally to be a initial variable for an optimization system having some constraints for its simulation to improve the performance of milling machine tool.

2.5. SPINDLE

LIU et al.[21] conclude the reason behind the spindle power loss is due the factors as Spindle is composed of mechanical and electrical transmission system where each component has several load loss, Heat generated in the spindle system and self load of the spindle, After installation the additional losses comes in to play, Difficulty in preparing mathematical model because of several unknown parameters.

To calculate spindle power loss they experimented under various conditions such that spindle speed, feed rate and cutting depth the power losses in spindle is always 15 to 20 % and maximum value reaches up to 30%.

2.6. CONCLUSION OF THE LITERATURE SURVEY

The conclusion from the literature survey extracted is that wood is highly anisotropic material with material properties vary in each direction of grains. Cutting properties vary from species to species and each species has its own mechanical property. To design CNC machine FEM modeling of each components is being done with its own boundary condition and results is studied and analyzed for optimization according to operation required. Moreover the analytical methods for the selection of components and to calculate the stability are also studied. The focus is done over the studying stability of machine tool is taken in the literature because of designing the precision machine for carving operation. The cutting methods and spindle selection is described with its challenges over the installation and the power loss in operation. The literature survey done was to find out the working methods and operational procedure towards the designing procedure.

CHAPTER: 3
EMPIRICAL RELATIONSHIP AND METHODOLOGY

To design a machine tool the factor to be considered is the nature of work to be performed from the machine. Here the current work is to design and optimize a wood sculpturing machine tool therefore Achieving precision is the most primary requirement of the design. Precision of a machine depends upon the tool path deviation from its original indented path. More is the deviation less will be the precision. The main cause of the tool path deviation is the deflection of the machine. Here in this chapter the empirical relations are described for designing the machine tool components, a step by step methodology is followed for the process. The important parameters which will influence the design are:

1. Nature of work material to be machined
2. Machining parameters such as depth of cut, width of cut, feed rate etc.
3. Span of the machine tool in X, Y and Z direction which depends upon the work material, this is the most important parameter which causes deflection in the machine tool.
4. Selection of proper factor of safety
5. Material selected for the machine tool components.
6. Availability of Standard components against the designed components and its effect on the other parameters.

The empirical relation are defined and calculated step by step staring from the force calculation which the machine tool is going to handle to the CNC component selection and its effect for the selection of other components. The optimization will be done after each step of the design in ANSYS after creating the CAD model in Creo Elements/ pro which will be discussed in chapter 4. The flow chart described in figure:3.1 shows the design step to be followed to reach the structural design of the whole system. The knowledge of machine design, machine tool and strength of material is considered at each step for selection and calculation.

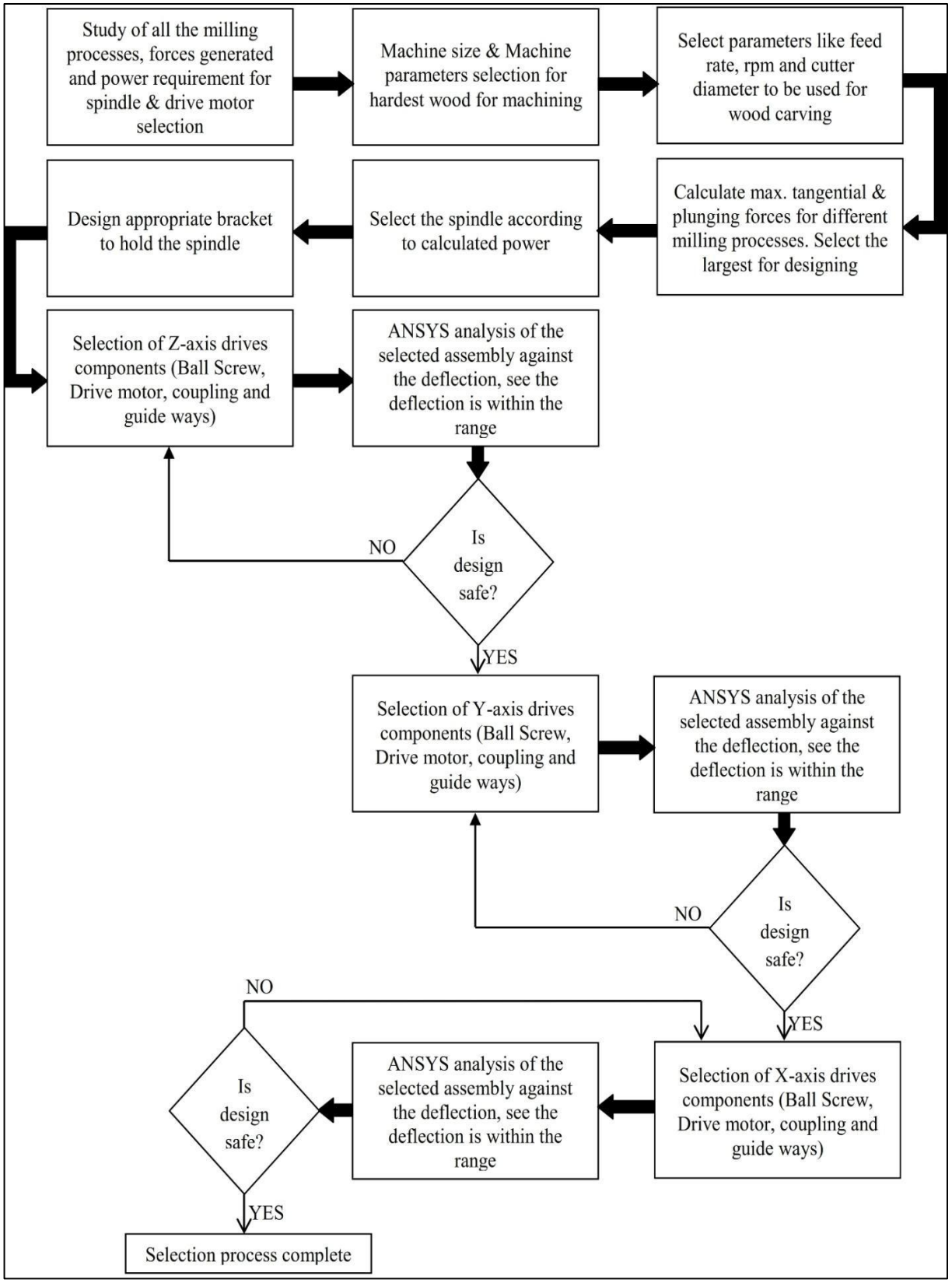

Figure 3.1: Flow chart for selection process of Machine tool

3.1.MILLING OPERATION FOR MATERIAL REMOVAL

Milling is the process of machining in which material is removed with the help of a tool rotating about its axis, the process is different from the drilling is apart from traveling linearly along its axis the milling tool travels perpendicular to its axis also.

3.1.1 End milling

In this process the cutter removes the material from the ends or sides of the work piece as shown in figure 3.2.

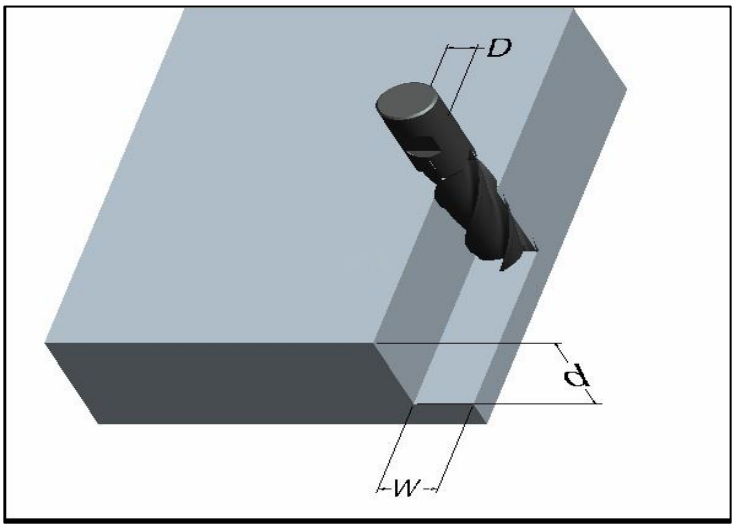

Figure 3.2: End milling

3.1.2 Face Milling

In face milling generally the top surface of the work piece is being machined. It is the most common type of milling operation for most of the sculpturing operations.

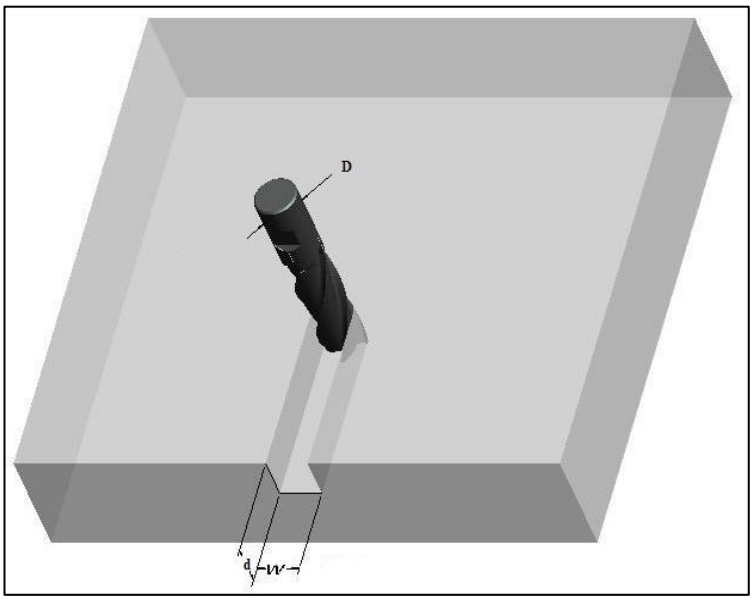

Figure 3.3: Face milling

Cutting force and machining Power required for face and end milling

The power can be calculated from the equation below:

$$P_f = \frac{K \times Q}{1000} \qquad \text{Eq.3.1}$$

Tangential cutting force and cutting speed are calculated by equation below:

$$F_t = \frac{(P \times 60000)}{Vc} \qquad \text{Eq 3.2}$$

$$V_c = \frac{(\pi \times D \times N)}{1000} \qquad \text{Eq 3.3}$$

Where,

P_f= power in face milling in kW

F_t= Tangential cutting force in N

V_c= cutting speed in m/min

K= coefficient - specific cutting power in W/m^3/min

Q= Material removal rate in m^3/min

D= Diameter of tool in mm

N= RPM of spindle

Material removal rate can be calculated from the formulas below

$$Q = \frac{d \times w \times f}{1000 \times 1000} \qquad \text{Eq 3.4}$$

3.1.3 Plunge milling

Plunging was invented to be able to remove large quantities of material and is especially adapted for applications where long overhang is needed, for example in 3D milling

Power in plunge milling can be calculated from the following relation:

$$P_p = \frac{(Kc \times D \times fz \times Vc)}{240000} \qquad \text{Eq 3.5}$$

And Thrust force

$$F_p = \frac{(k\prime \times Kc \times fz \times D)}{2} \qquad \text{Eq 3.6}$$

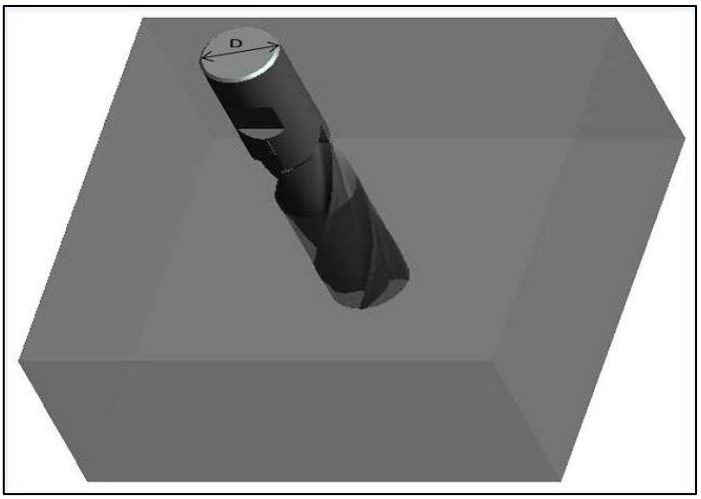

Figure 3.4: Plunge milling

Where, Pp= power for plunge milling in kW

Fp= Thrust force in plunge milling in N

K'=coefficient of Geometry of the tip of the tool

Kc= Specific cutting force in N/m^2

fz= Feed per tooth in m/tooth.

3.2 SPINDLE MOTOR SELECTION

Following points should be considered while selecting the spindle motor for the machine:

(i) It should run at high Rpm such that to cut brittle material like wood.

(ii) Should be air cooled instead of water cooled to avoid any moisture on wood.

(iii) Depth and the width of cut should be known.

(iv) Feed rate.

(v) Diameter of the cutting tool.

The selection of spindle power is followed by the calculation of tangential and axial force on work material required to make machining. And these forces depend on the specific cutting force of the material and method of machining. In vertical milling process the two types of forces tangential and axial occurs due to simple milling and plunging respectively. While machining wood the knowledge of specific cutting force becomes very difficult because of the following reasons:

1. Wood variety varies from very soft wood to very hard wood.

2. Seasoning of wood improves its material properties which depend upon time and method of seasoning

3. Properties of wood not same in all direction.

Therefore specific cutting force of Aluminum is considered instead of wood having similar machining properties. Both the material shows brittle behavior while machining and for the design safety the value of aluminum is safer to use instead of wood

3.3 DESIGN OF SPINDLE MOUNTING BRACKET

The bracket is required to hold the spindle upon which all cutting forces are acting. Therefore followings things are required to be selected and designed:

(i) Material of the bracket plate.

(ii) Number of bolts required to hold the bracket and spindle

(iii) Pitch of the bolt and side margin against the bearing (tearing) strength of bracket (thickness of the bracket plate).

(iv) Diameter of bolt.

(v) Material of the bolt and Nut.

Design criteria is based upon on various types of forces acting on the spindle as studied in machine design textbook for bolt design[36] which has been explained below

Case1: When cutting along X-axis (Load acting parallel to the axis of bolt)

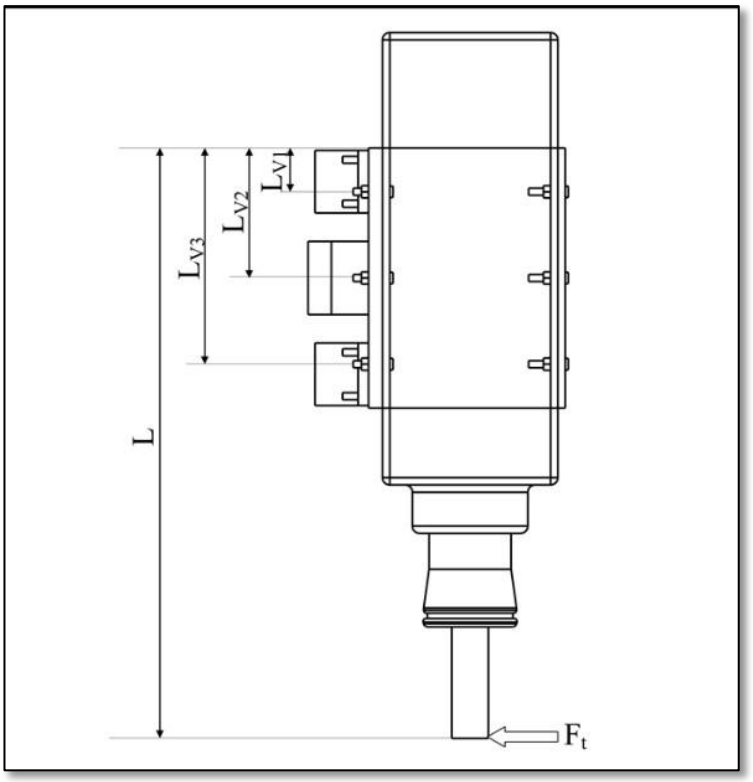

Figure 3.5: Distances of bolt from tilting edge when cutting along X-axis

Inertia load can be calculated by the formula given as:

$W_i = m_{asm1} \times \alpha$ Eq 3.7

Total load acting on the bolt

$$W = W_i + F_t \quad \text{Eq 3.8}$$

Where, W_i = inertia load in N

W = total load acting on bolts in N

m_{asm1}= Mass of the spindle and bracket in kg

α = Acceleration of motor in m/sec^2

Let,

N_b =Number of bolt

Therefore, Direct Tensile load on each bolt is calculated using equation 3.8

$$W_{dt} = \frac{W}{N_b} \quad \text{Eq 3.9}$$

W_{dt}= Direct tensile load in N

Now,

Distance of bolt in a row from tilting edge=L_{v1} in m

Distance of bolt in another row from tilting edge= L_{v2} in m

Distance of bolt in another row from tilting edge= L_{v3} in m

Distance of the force from the tilting edge =L in m

Load on the bolt per unit distance in N/m calculated using equation 3.8

$$wb = \frac{W \times L}{2({L_{v1}}^2 + {L_{v2}}^2 + {L_{v3}}^2)} \quad \text{Eq 3.10}$$

Tensile load on each bolt at distance L_{v1} in N

$$W_{t1} = \text{w} \times L_{v1} \quad \text{Eq 3.11}$$

Tensile load on each bolt at distance L_{v2} in N

$$W_{t2} = \text{w} \times \text{L}_{\text{v2}} \quad \text{Eq 3.12}$$

Tensile load on each bolt at distance L_{v3} in N

$$W_{t3} = \text{w} \times \text{L}_{\text{v3}} \quad \text{Eq 3.13}$$

Total tensile load on bolt at distance L_{v1} in N

$$W_1 = W_{dt} + W_{t1} \quad \text{Eq 3.14}$$

Total tensile load on bolt at distance L_{v2} in N

$$W_2 = W_{dt} + W_{t2}$$ Eq 3.15

Total tensile load on bolt at distance L_{v3} in N

$$W_3 = W_{dt} + W_{t3}$$ Eq 3.16

Maximum Tensile load (W_{mtb}) will be chosen from the equations 3.14, 3.15, 3.16 at different length

Now the Diameter of the bolt can be calculated from the formula given below

$$W_{mtb} = \frac{\pi}{4}(d_c)^2\sigma_{bolt}$$ Eq 3.17

Where σ_{bolt} = allowable tensile stress for bolt material in N/m^2

Case2: When cutting in Y-axis (Load acting in the plane containing the bolt)

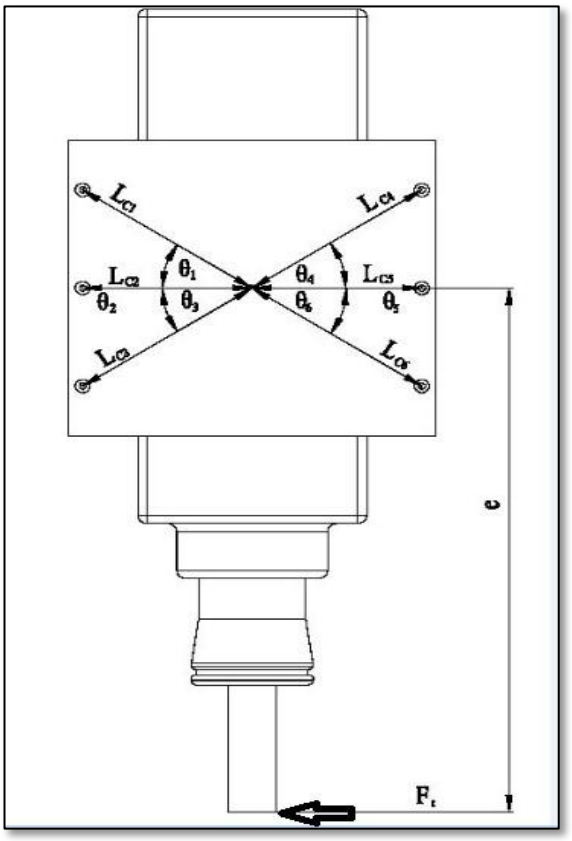

Figure 3.6: Distances of bolt from center when cutting along Y-axis

Load acting on the joints = W in N

Eccentricity of the load= e in m

Number of bolt = N_b

Direct shear load on each rivet

$$W_s = \frac{W}{N_b}$$ Eq 3.18

Turning moment produced by the load P due to eccentricity

$$M_{ie} = W \times e$$ Eq. 3.19

Let

Distance of 1st bolt from centroid of sub assembly 1= l_{c1} in m

Distance of 2nd bolt from centroid of sub assembly 1= l_{c2} in m

Distance of 3rd bolt from centroid of sub assembly 1= l_{c3} in m

Distance of 4th bolt from centroid of sub assembly 1= l_{c4} in m

Distance of 5th bolt from centroid of sub assembly 1= l_{c5} in m

Distance of 6th bolt from centroid of sub assembly 1= l_{c6} in m

Then secondary shear load can be calculated as:

Secondary shear load on bolt 1(S_{fb1}) $= \frac{(M_{ie}) \times l_{c1}}{l_{c1}^2 + l_{c2}^2 + l_{c3}^2 + l_{c4}^2 + l_{c5}^2 + l_{c6}^2}$ Eq 3.20

Secondary shear load on bolt 2(S_{fb2}) $= \frac{(M_{ie}) \times l_{c2}}{l_{c1}^2 + l_{c2}^2 + l_{c3}^2 + l_{c4}^2 + l_{c5}^2 + l_{c6}^2}$ Eq 3.21

Secondary shear load on bolt 3(S_{fb3}) $= \frac{(M_{ie}) \times l_{c3}}{l_{c1}^2 + l_{c2}^2 + l_{c3}^2 + l_{c4}^2 + l_{c5}^2 + l_{c6}^2}$ Eq 3.22

Secondary shear load on bolt 4(S_{fb4}) $= \frac{(M_{ie}) \times l_{c4}}{l_{c1}^2 + l_{c2}^2 + l_{c3}^2 + l_{c4}^2 + l_{c5}^2 + l_{c6}^2}$ Eq 3.23

Secondary shear load on bolt 5(S_{fb5}) $= \frac{(M_{ie}) \times l_{c5}}{l_{c1}^2 + l_{c2}^2 + l_{c3}^2 + l_{c4}^2 + l_{c5}^2 + l_{c6}^2}$ Eq 3.24

Secondary shear load on bolt 6(S_{fb6}) $= \frac{(M_{ie}) \times l_{c6}}{l_{c1}^2 + l_{c2}^2 + l_{c3}^2 + l_{c4}^2 + l_{c5}^2 + l_{c6}^2}$ Eq 3.25

Angle between direct and secondary shear load for bolt 1=cosθ1

Angle between direct and secondary shear load for bolt 2=cosθ2

Angle between direct and secondary shear load for bolt 3=cosθ3

Angle between direct and secondary shear load for bolt 4=cosθ4

Angle between direct and secondary shear load for bolt 5=cosθ5

Angle between direct and secondary shear load for bolt 6=cosθ6

Resultant shear load on bolt 1(R1) $= \sqrt{W_s^2 + S_{fb1}^2 + 2W_s S_{fb1} cos\theta 1}$ Eq 3.26

Resultant shear load on bolt 2(R2) $= \sqrt{W_s^2 + S_{fb2}^2 + 2W_s S_{fb2} cos\theta 2}$ Eq 3.27

Resultant shear load on bolt 3(R3) = $\sqrt{{W_s}^2 + {S_{fb3}}^2 + 2W_s S_{fb3} cos\theta 3}$ Eq 3.28

Resultant shear load on bolt 4(R4) = $\sqrt{{W_s}^2 + {S_{fb4}}^2 + 2W_s S_{fb4} cos\theta 4}$ Eq 3.29

Resultant shear load on bolt 5(R5) = $\sqrt{{W_s}^2 + {S_{fb5}}^2 + 2W_s S_{fb5} cos\theta 5}$ Eq 3.30

Resultant shear load on bolt 6(R6) = $\sqrt{{W_s}^2 + {S_{fb6}}^2 + 2W_s S_{fb6} cos\theta 6}$ Eq 3.31

Maximum Resultant Shear load(R_S) will be from these above six equations

Hence Diameter of bolt can be calculated as

$R_S = \frac{\pi}{4} {d_{by}}^2 \tau_{bolt}$ Eq 3.32

Where τ_{bolt} =maximum permissible shear stress of the bolt material in N/m^2

R_S= maximum resultant shear load inN

d_{by} = diameter of bolt in shearing in m

Case 3. When cutting in Z-axis vertically downwards direction (cutting load acting perpendicular to the Bracket bolts)

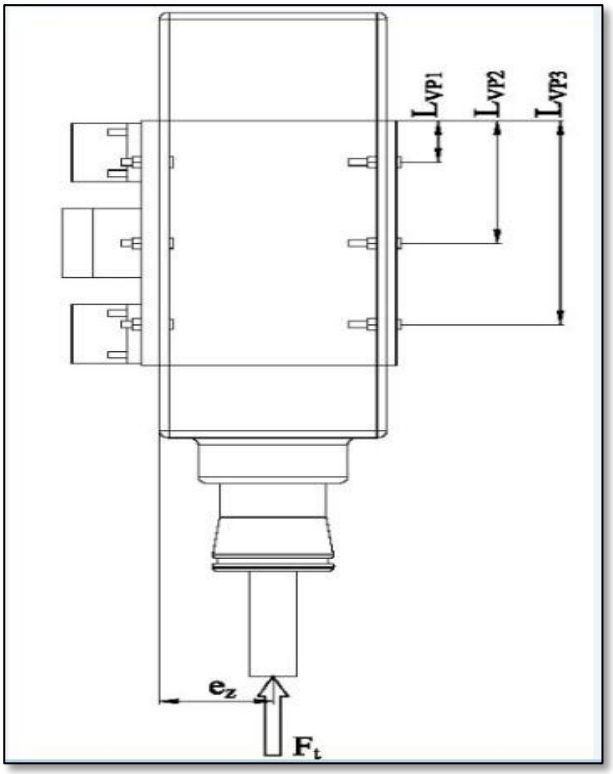

Figure 3.7: Distances of bolt from tilting edge when cutting along Z-axis

Load on clamping bolts in plunge cutting

$W_P = W_i + F_p$ Eq 3.33

Where W_i = Inertia load in N

F_p = plunge Force in N

Direct shear load on each bolt

$$W_{ds} = \frac{W_P}{N_b} \quad \text{Eq 3.34}$$

Vertical distance of bolts in first row from twisting edge = L_{v1} in m

Vertical distance of bolts in second row from twisting edge =L_{v2} in m

Vertical distance of bolts in third row from twisting edge = L_{v3} in m

Bolt at maximum Vertical distance from twisting edge = L_t in m

Maximum tensile load on bolt (Wt)

$$W_t = \frac{W_{ds} \times e_z \times L_t}{2(L_{v1}^2 + L_{v2}^2 + L_{V3}^2)} \quad \text{Eq 3.35}$$

Where e_z = Eccentricity of load in m

Equivalent tensile Load (W_{te})

$$W_{te} = \frac{1}{2}(W_t + \sqrt{W_t^2 + 4W_{ds}^2}) \quad \text{Eq 3.36}$$

Equivalent shear Load (W_{se})

$$W_{se} = \frac{1}{2}\sqrt{W_t^2 + 4W_{ds}^2}) \quad \text{Eq 3.37}$$

Diameter of the bracket clamping bolt in tension (d_{btz})

$$W_{te} = \frac{\pi}{4}(d_{btz})^2 \sigma_{bolt} \quad \text{Eq 3.38}$$

Diameter of the bracket bolt according to shearing (d_{bsz})

$$W_{Se} = \frac{\pi}{4} d_{bsz}{}^2 \tau_{bolt} \quad \text{Eq 3.39}$$

Case 4. Check against tearing of bracket plate

The tearing of bracket plate can occur due to the diameter of the bolt and the thickness of the bracket plate

The allowable bearing stress in the Bracket plate

$$\sigma_{bcalculated} \frac{F_m}{d_b \times B_t} \quad \text{Eq 3.40}$$

Where, F_m= Maximum cutting force from tangential and plunge in N

d_b= diameter of bolt selected from above three cases in m

B_t= thickness of the bracket plate in m

3.4 SELECTION OF BALL SCREW.

A ball screw is the machine tool member which transmits rotary motion from the drive motor to the linear motion to the slide way.

(i) It is subjected to the thrust or axial force due to the load of work piece, cutting force, friction of the slide way and inertia force.
(ii) Torsion force to overcome this force.

When the nature of the stress is not unidirectional and combination of stresses are acting on a component it will be calculated from Von- mises stress formula[37]. The equivalent von-mises stress is composed of axial and Torsional stress in case of ball screw which can be calculated by the relation given below

- **Axial stress**

$$\sigma_{axial} = \frac{F_a}{\pi \times r_b{}^2} \quad \text{Eq 3.41}$$

Where, σ_{axial} = axial stress in N/m^2

F_a= Axial load applied on the Ball Screw in N

r_b = Root Radius of the ball screw in m

- **Torsional stress**

$$\tau_{torsional} = \frac{2 \times T_t}{\pi \times r_b{}^3} \quad \text{Eq 3.42}$$

Where, $\tau_{torsional}$ = Torsional stress in N/m^2

T_t= Driving torque to obtain thrust force in N-m

Therefore, **Equivalent Von-mises stress**

$$\sigma_{eq} = \sqrt{\sigma_{axial}^2 + 3\tau_{torsinal}^2} \quad \text{Eq 3.43}$$

The formulae to calculate the axial load and driving torque are as follows

Axial load applied on the ball screw

a) In vertical mount (Z-axis)

$$F_{a1} = (m \times g) + F_{fR} + (m \times \alpha) - F_p \quad \text{Eq 3.44}$$

$$F_{a2} = (m \times g) + F_{fR} - F_p \quad \text{Eq 3.45}$$

$$F_{a3} = (m \times g) + F_{fR} - (m \times \alpha) - F_p \quad \text{Eq 3.46}$$

$$F_{a4} = (m \times g) - F_{fR} - (m \times \alpha) \quad \text{Eq 3.47}$$

$$F_{a5} = (m \times g) - F_{fR} \quad \text{Eq 3.48}$$

$$F_{a6} = (m \times g) - F_{fR} + (m \times \alpha) \quad \text{Eq 3.49}$$

b) In side mount (Y-axis)

$$F_{a1} = (m \times g) + F_{fR} + (m \times \alpha) + F_t \quad \text{Eq 3.50}$$

$$F_{a2} = (m \times g) + F_{fR} + F_t \quad \text{Eq 3.51}$$

$$F_{a3} = (m \times g) + F_{fR} - (m \times \alpha) + F_t \quad \text{Eq 3.52}$$

$$F_{a4} = (m \times g) - F_{fR} - (m \times \alpha) + F_t \quad \text{Eq 3.53}$$

$$F_{a5} = (m \times g) - F_{fR} + F_t \quad \text{Eq 3.54}$$

$$F_{a6} = (m \times g) - F_{fR} + (m \times \alpha) + F_t \quad \text{Eq 3.55}$$

c) In horizontal mount (X-axis)

$$F_{a1} = \big(\mu \times (m \times g)\big) + F_{fR} + (m \times \alpha) + F_t \quad \text{Eq 3.56}$$

$$F_{a2} = \big(\mu \times (m \times g)\big) + F_{fR} + F_t \quad \text{Eq 3.57}$$

$$F_{a3} = \big(\mu \times (m \times g)\big) + F_{fR} - (m \times \alpha) + F_t \quad \text{Eq 3.58}$$

$$F_{a4} = \big(\mu \times (m \times g)\big) - F_{fR} - (m \times \alpha) + F_t \quad \text{Eq 3.59}$$

$$F_{a5} = \big(\mu \times (m \times g)\big) - F_{fR} + F_t \quad \text{Eq 3.60}$$

$$F_{a6} = \big(\mu \times (m \times g)\big) - F_{fR} + (m \times \alpha) + F_t \quad \text{Eq 3.61}$$

Where

F_{a1} = Axial load during forward acceleration in N

F_{a2} = Axial load during forward uniform motion in N

F_{a3} = Axial load during forward deceleration in N

F_{a4} = Axial load during backward acceleration in N

F_{a5} = Axial load during backward uniform motion in N

F_{a6} = Axial load during backward deceleration in N.

m= Transferred mass in kg.

F_{fR} = guide surface resistance in N

F_p =Thrust Force in N

μ = Friction coefficient of guide surface

The value of maximum axial load should be selected for the design.

Ball screw selection is based upon the parameters selected for the drive motor which runs the ball screw to transmit the motion.

3.5 SELECTION OF SLIDEWAY.

The round shaft slide way was selected earlier for the purpose of wood carving CNC machine because of its properties discussed. The selection of round shaft slide way depends upon the permissible value of bending moment. The models for the round shaft slide ways were taken from the round shaft guide way technology [31]

Calculation for the Bending Moment Produced

Bending moment = (cutting force) × (Distance of cutting force from the center of gravity of the arrangement)

3.5.1 Z-axis slide

The Z-axis slide way carries the spindle and the bracket arrangement and is under the direct effect of the cutting force. The Z-axis slide has to move very rapidly and is under motion in every process.

a) Bending moment along X-axis

(i) When cutting in Y-axis

$$M_X = F_t \times l_{ty} \quad \text{Eq. 3.62}$$

Where, F_t = Tangential cutting force in N

L_{ty}= Distance between cutting force and center of back plate along Z in m

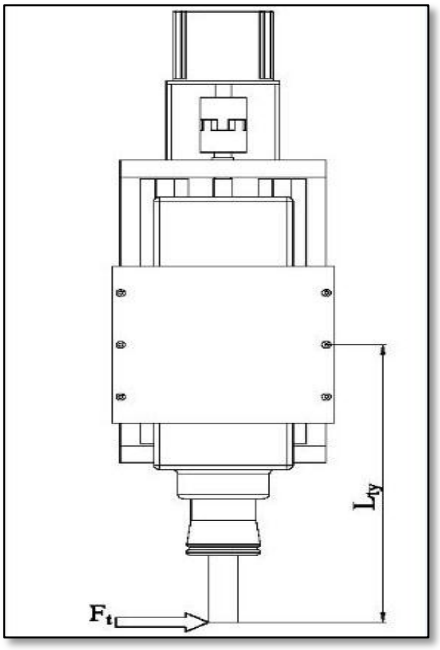

Figure 3.8: Distance between tangential Cutting force and center of back plate for Z –axis slide

b) Bending moment along Y-axis

(i) When cutting in X-axis

$$M_Y = F_t \times l_{tx}$$ Eq. 3.63

Where, L_{tx}= Distance between cutting force and farthest bearing block along Z in m

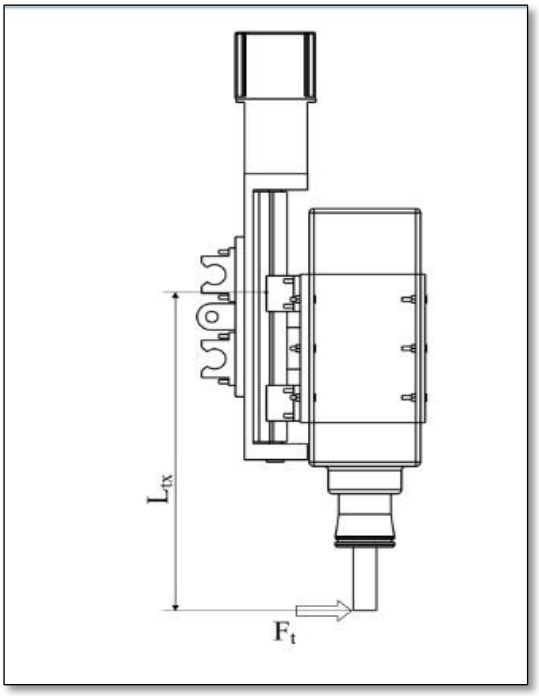

Figure 3.9: Distance between tangential Cutting force and farthest bearing for Z –axis slide

(ii) When cutting in Z- axis

$$M_Y = \left(F_p - W_{asm1}\right) \times l_{pz}$$ Eq. 3.64

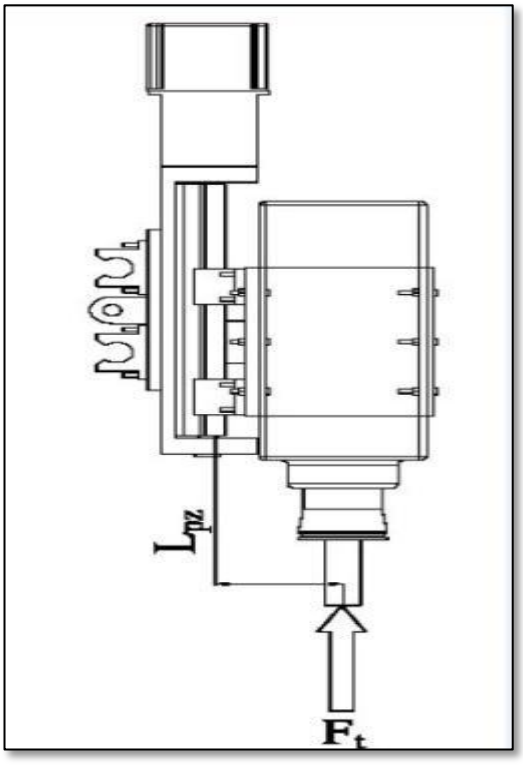

Figure 3.10: Distance between plunge force and center of bearing for Z –axis slide

Where,

F_p = Plunge force in N

W_{asm1}= weight of subassembly 1 of spindle and bracket in N

L_{pz}= Distance between plunging force and center of bearing along X

3.5.2 Y-axis slide

Selection of Y-axis slide is most critical in terms of deflection because it is the case of simply supported beam with large span length. The selection of the Y-axis slide is done without considering the self weight of the components whose analysis is done in ANSYS.

a) Bending moment along X-axis

When cutting in Y-axis

$$M_X = F_t \times l_{ty} \quad \text{Eq. 3.65}$$

Where, F_t = Tangential cutting force in N

L_{ty}= Distance between cutting force and center of back plate along Z in m

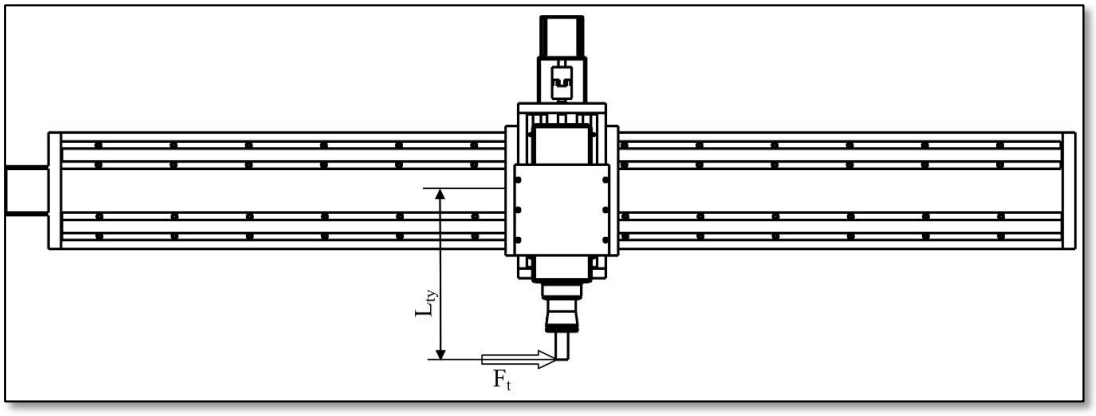

Figure 3.11: Distance between tangential Cutting force and center of back plate for Y –axis slide

b) Bending moment along Y-axis

(i) When cutting in X-axis

$$M_Y = F_t \times l_{tx} \quad \text{Eq. 3.66}$$

Where ,L_{tx} = Distance between cutting force and farthest bearing block along Z in m

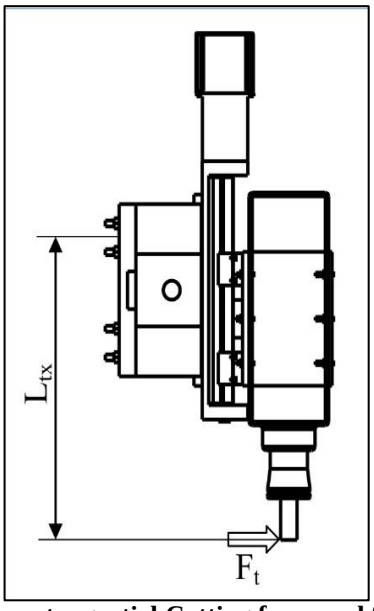

Figure 3.12: Distance between tangential Cutting force and farthest bearing for Y –axis slide

(ii) When cutting in Z- axis

Eq. 3.67

$$M_y = (F_P - W_{asm1}) \times l_{pz}$$

Where,

F_p = Plunge force in N

W_{asm1}= weight of subassembly 1 of spindle and bracket in N

L_{pz}= Distance between plunging force and center of bearing along X

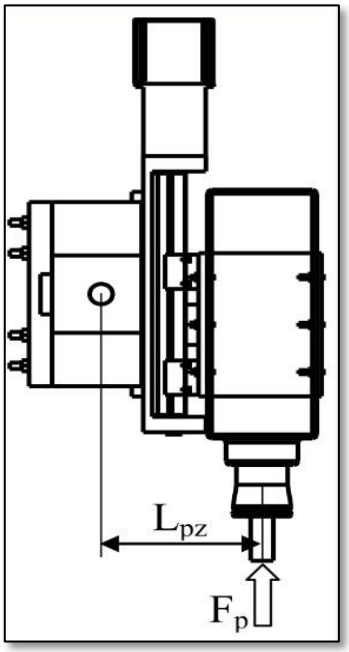

Figure 3.13: Distance between plunge force and center of bearing for Y –axis slide

3.5.3 X-axis Slide

X –axis slide will be the longest among all the drives which are not under any moment but comes under the direct load.

3.6 SELECTION OF DRIVING MOTOR

For the selection of proper motor and its size the torque required should be calculated, for which these point should be considered while calculating the required motor torque

(i) Rate of acceleration, deceleration and required velocity for the desired motion.

(ii) Inertia, frictional and other load torques to be encountered.

(iii) Condition and Environment of operation.

Total peak torque can be calculated as the sum of all the torque which machine has to overcome as given below

$$Tp = T_\alpha + T_f + T_\omega + T_g \qquad \text{Eq. 3.68}$$

Where,

T_α =Acceleration torque in N-m

T_f = Friction torque in N-m

T_ω = Viscous torque in N-m

T_g =Gravity torque in N-m

3.6.1 Acceleration torque

Also named as pull up torque it is called as acceleration torque because at this moment speed changes from zero to maximum velocity.

$$T\alpha = \frac{Jt \times \alpha}{e} \qquad \text{Eq. 3.69}$$

Where, Jt = Total inertia in kg/m^2

α = Angular Acceleration in rad/sec^2

e= Transmission efficiency

Total inertia can be calculated by the formulae given below:

$$Jt = J1 + \frac{N1}{N2^2}^2 (J2 + J3) + J4 \qquad \text{Eq. 3.70}$$

Where, *J1*=inertia of pinion in kg/m^2

J2=inertia of gear in kg/m^2

J3= inertia of feed screw in kg/m^2

J4=inertia of table and work piece. in kg/m^2

Calculation of all various inertia components are given below

$$J3 = \frac{\pi L \rho {r_b}^4}{2} \quad \text{Eq. 3.71}$$

$$J_4 = m_{asm2} \times (l_b)^2 \quad \text{Eq.3.72}$$

3.6.2 Friction torque

It is the torque caused by the frictional force between the two objects in contact move.

$$Tf = \frac{W\mu}{2\pi Pe} \quad \text{Eq. 3.73}$$

Where, μ= Co-efficient of friction

P= Pitch of feed screw

3.6.3 Gravity torque

Gravity torque is the torque required to overcome the gravitational force in usually Z-axis drives

$$\text{Tg} = \frac{0.0016\text{W}}{\text{Pe}} \quad \text{Eq. 3.74}$$

3.7 SELECTION OF THE COUPLING

The coupling should require transmitting the torque from drive motor to the ball screw shaft. Therefore coupling should be designed to withstand the required and fluctuating torque. The

Selection procedure followed for selection of couplings are mention below[38]:

Rated torque of the coupling(T_{kn})

$$T_{KN} = T_{pc} \times S_d \times S_t \quad \text{Eq.3.75}$$

Where, Tpc= Peak torque in N-m

S_d= Torsional Stiffness factor

S_t= Temperature effect

$$T_{PC} = T_{AS} \times m_{AL} \times S_A \quad \text{Eq. 3.76}$$

Where, T_{AS}= Maximum Driving torque in N-m

m_{AL}= Rotational inertia co-efficient of load side

S_A= Operating Factor

$$m_{AL} = \frac{J_L}{J_A + J_L} \quad \text{Eq. 3.77}$$

Where J_L=Mass Moment of inertia of load side in kgm^2

J_A=Mass Moment of inertia of driving side in kgm^2

$$J_A = J_{MOT} + \frac{1}{2} J_K \quad \text{Eq. 3.78}$$

$$J_L = J_{Schl} + \frac{1}{2} J_K + J_{bs} \quad \text{Eq. 3.79}$$

Where, J_{MOT}= Mass Moment of inertia of Motor in kgm^2

J_K = Mass Moment of inertia of Coupling in kgm^2

J_{bs}= Mass Moment of inertia of ball screw in kgm^2

J_{SChl}= Mass Moment of inertia of slide and work piece in kgm^2

The mass moment of inertia of slide and work piece can be calculated from the formula given below:

$$J_{Schl} = m_{Schl} \times (l)^2 \quad \text{Eq. 3.80}$$

Where m_{SChl} = Mass of slide and work piece in kg

l= Screw pitch in m

3.8 CONCLUSION OF THE METHODOLOGY

From the methodology discussed in this chapter the design process comprises of the following things:

(i) Cutting force is calculated against the hardest wood material and the cutting parameters.

(ii) Suitable power of spindle is being selected with the design of the bracket to hold the spindle.

(iii) The slide way is the key component for selection as it is under maximum deflection. Here selection of Slide way is done without considering the self weight of the system which will be overcome in chapter 4 while analyzing the results coming out from the empirical relationship.

(iv) The effect of cutting force magnitude and direction will be considered only analytically.

(v) The ball screw and motor are selection for different drives were different considering the acceleration and guide surface friction.

CHAPTER 4

RESULTS AND DISCUSSION

The methodology described in chapter 3 has been used to design the initial dimension of the components. An Excel sheet is designed for study of design parameter variation with change in input parameter. The iteration is done in ANSYS to validate the results coming out from these relationship based upon which 3D CAD models are generated by applying the necessary boundary conditions and a safe model is selected.

The initial parameters set for the designing the machine tool is the operating parameters upon which the selection of the machine tool components depends critically. Following table shows the initial parameters taken for the design.

Table 4.1: Operating parameter for the design of machine tool

Parameters	Symbol	Value	Unit
Maximum Length of Tool	L_T	55	mm
Maximum Diameter of tool	D	25.4 mm	mm
Maximum Depth of cut	d	10 mm	mm
Maximum Feed rate	f	1.5	m/min
Maximum width of cut	w	25.4 mm	mm
Maximum Spindle rpm	N	18000	
Maximum acceleration for X, Y and Z-axis drives	α	0.660	m/sec^2
Length of Z-axis Traverse	L_z	304.8	mm
Length of Y-axis Traverse	L_y	2032	mm
Length of X-axis Traverse	L_x	2438	mm
Specific cutting force	K_c	17000000	N/m^2
Specific cutting power	K	1020000000	$W/m^3/min$

4.1. CUTTING FORCE AND POWER REQUIREMENT.

a) Face and end milling

Based upon the empirical relationship in chapter 3, the value for power, tangential cutting force ,cutting speed and material removal rate are given below calculating using the equation number 3.1,3.2,3.3,3.4 respectively

Table 4.2: value of cutting forces and power in face and end milling

Parameter	Symbol	value	unit
Cutting speed	V_C	1435.6080	m/min
Material removal rate	Q	0.0004	m3/min
Tangential cutting force (used for X and Y-axis drive motor selection)	F_t	270.7006	N
Minimum spindle power required	P_f	6.4770	kW

b) Plunge milling

For plunge milling the value of cutting speed, spindle power requirement and thrust force are calculated by using the equation number 3.3, 3.4, 3.5 respectively

Table 4.3: value of cutting forces and power in plunge milling

Parameter	Symbol	value	unit
Cutting speed	V_C	1435.6080	m/min
Thrust force (used for Z-axis drive motor selection)	F_p	269.8750	N
Minimum spindle power required	P_p	6.4572	kW

From the above two milling processes the power is coming out to be Maximum for face and end milling.

4.2. SPINDLE SELECTION

The power coming out to be Maximum from milling or plunging should be selected. The spindle power should be more than the calculated power by a factor of 10-30 % [21]

Select the nearest available spindle from the market. The following data should be noted down:

(i) Maximum available Rpm of the spindle.

(ii) Weight of the spindle unit.

(iii) Maximum Torque available.

The spindle power requirement comes out to 6.5 kW but the actual spindle power requirement is more because of the loss factor as discussed earlier which occurs in the spindle that is between 10 to 30 % larger than the calculated .so the actual spindle power comes out

nearly 8 kW. The available spindle from the market was picked with its drawing and specification for generating the Cad model and analysis.

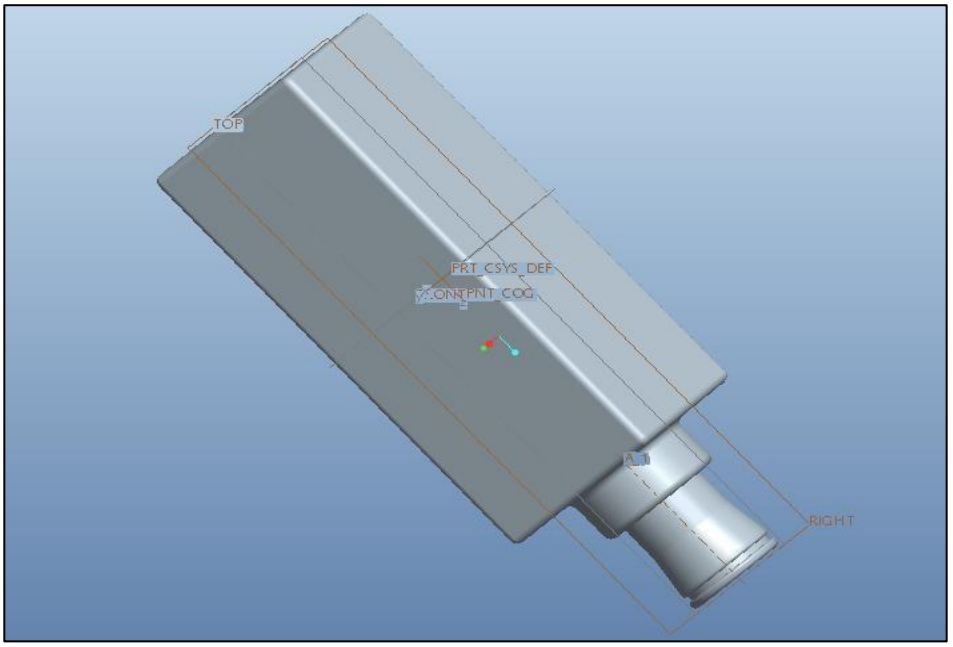

Figure 4.1: Cad model of selected Spindle

Table 4.4: specification of the standard spindle selected

Parameter	**Value**	**Unit**
Voltage	380	*V*
Power	8	*kW*
Speed	18000	*Rpm*
Frequency	300	*HZ*
Current	26.5	*A*
Collect radius	32	*mm*
Mass	32	*kg*

4.3. BRACKET DESIGN

For the design of bracket the consideration taken is

(i) The diameter of bolts which holds the bracket with back plate

(ii) Thickness of the bracket plate

The material for the bracket was taken as Aluminum 6061O and for the bolt stainless steel

Table 4.5: Mechanical properties of the Aluminum 6061O[39]

Density	2700 Kg/m^3
Young's Modulus	68.9 GPa
Poisson's ratio	0.33
Ultimate tensile strength	124 MPa
Ultimate Yield Strength	55.2 Mpa
Ultimate Bearing Strength	228 MPa

Table 4.6: Mechanical properties of the stainless steel[39]

Density	7750 kg/m^3
Young's modulus	193 GPa
Poisson's ratio	0.31
Ultimate Tensile Strength	586 MPa
Ultimate Yield Strength	207 MPa

4.3.1. Calculation for the bolt diameter

The diameter of bolt can be calculated analytically by the help of empirical relationships under different direction of loading conditions while the thickness of bracket plate will be optimize with the help of FEM model analysis in ANSYS.

Table 4.7: Initial parameters for bolt diameter calculation

parameter	symbol	value
Mass of subassembly 1	M_{asm1}	37 kg
Number of bolts	N_b	06
Factor of safety for clamp bolts	S_b	06

Case1: When cutting in along X-axis (Load acting parallel to the axis of bolt)

The calculation for bolt diameter when cutting operation is done in x-axis will be against the tensile stress produced on the bolts. The dimensions will be taken from the Cad model generated for spindle and bracket considering the distances L_{v1}, $L_{v2,}$ Lv_3 and L shown in the figure: 4.2 and the various loads on the bolt will be calculated using the relationship 3.7 to 3.16. The safe diameter of bolt will be calculated considering the factor of safety 6 and from the relationship 3.17

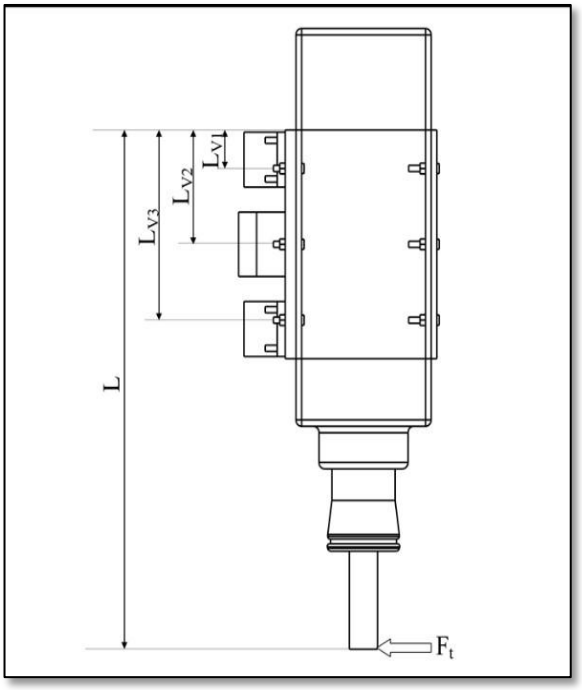

Figure 4.2: Distances of bolt from tilting edge when cutting along X-axis

Table 4.8: Value for bolt diameter for cutting along X-axis

Parameter	Symbol	Value	Unit
Vertical distance of bolts in first row from twisting edge	L_{v1}	0.0300	m
Vertical distance of bolts in second row from twisting edge	L_{v2}	0.0889	m
Vertical distance of bolts in third row from twisting edge	L_{v3}	0.1478	m
Distance of the force vector from the twisting edge	L	0.3823	m
Total load acting on each bolt	W	273.1426	N
Direct Tensile load on each bolt	W_{dt}	45.5238	N
Load on the bolt per unit distance	w_b	1703.3510	N
Tensile load on each bolt at distance Lv1	W_{t1}	51.1005	N
Tensile load on each bolt at distance Lv2	W_{t2}	151.4279	N
Tensile load on each bolt at distance Lv3	W_{t3}	251.7553	N
Total tensile load on bolt at distance Lv1	W_1	96.6243	N
Total tensile load on bolt at distance Lv2	W_2	196.9517	N
Total tensile load on bolt at distance Lv3	W_3	297.2790	N
Maximum tensile load on group of bracket clamping bolts	W_{mtb}	297.2790	N
Diameter of the bracket clamping bolt	d_{bx}	2.0	mm

Case2: When cutting along Y-axis (Load acting in the plane containing the bolt)

While cutting in Y-axis the bolt will be under shear load. The bolts will be tends to shear off from the plate and bracket surface. The dimensions will be taken from the Cad model generated for spindle and bracket considering the distances L_{c1}, $L_{c2,}$ L_{c3}, L_{c4}, $L_{c5,}$ L_{c6}, eccentricity e_z and angle Θ_1, $\Theta_{2,}$ $\Theta_{3,}$ $\Theta_{4,}$ $\Theta_{5,}$ Θ_6 shown in the figure:4.3 and the various loads on the bolt will be calculated using the relationship 3.18 to 3.31. The safe diameter of bolt will be calculated considering the factor of safety 6 and from the relationship 3.32

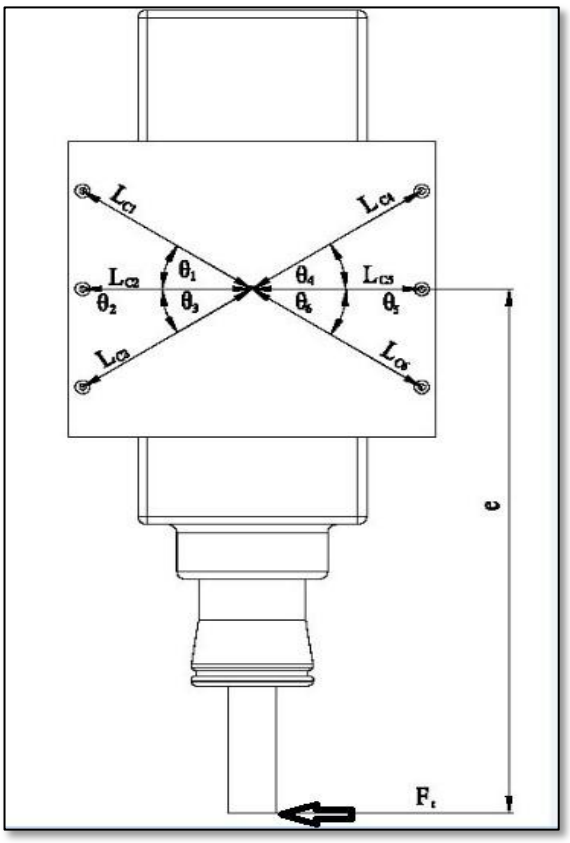

Figure 4.3: Distances of bolt from center when cutting along Y-axis

Table 4.9: Value for bolt diameter for cutting along Y-axis

Parameter	Symbol	Value	Unit
Eccentricity of the load	e_y	0.2930	m
Direct shear load on each bolt	Ws	45.5238 N	N
Turning moment produced by the load *W* due to eccentricity	M_{ie}	80.03 N-m	N-m
Distance of 1st bolt from centroid	L_{c1}	0.1065	m
Distance of 2nd bolt from centroid	L_{c2}	0.0887	m
Distance of 3rd bolt from centroid	L_{c3}	0.1065	m
Distance of 4th bolt from centroid	L_{c4}	0.1065	m

Distance of 5th bolt from centroid	L_{c5}	0.0887	m
Distance of 6th bolt from centroid	L_{c6}	0.1065	m
secondary shear load on bolt 1	S_{fb1}	139.5063	N
secondary shear load on bolt 2	S_{fb2}	116.2225	N
secondary shear load on bolt 3	S_{fb3}	139.5063	N
secondary shear load on bolt 4	S_{fb4}	139.5063	N
secondary shear load on bolt 5	S_{fb5}	116.2225	N
secondary shear load on bolt 6	S_{fb6}	139.5063	N
Angle between direct and secondary shear load for bolt 1	$cos\theta 1$	0.8330	
Angle between direct and secondary shear load for bolt 2	$cos\theta 2$	1.0000	
Angle between direct and secondary shear load for bolt 3	$cos\theta 3$	0.8330	
Angle between direct and secondary shear load for bolt 4	$cos\theta 4$	0.8330	
Angle between direct and secondary shear load for bolt 5	$cos\theta 5$	1.0000	
Angle between direct and secondary shear load for bolt 6	$cos\theta 6$	0.8330	
Resultant shear load on bolt 1	R_{S1}	177.3182	N
Resultant shear load on bolt 2	R_{S2}	161.7462	N
Resultant shear load on bolt 3	R_{S3}	177.3182	N
Resultant shear load on bolt 4	R_{S4}	177.3182	N
Resultant shear load on bolt 5	R_{S5}	161.7462	N
Resultant shear load on bolt 6	R_{S6}	177.3182	N
Maximum Resultant Shear load	R_S	177.3182	N
Diameter of bolt	d_{by}	2.2	mm

Case 3. When cutting along Z-axis vertically downwards direction (cutting load acting perpendicular to the Bracket bolts)

In case of plunge cutting the bolts will come under combination of tensile and shear stress. The distances L_{V1}, $L_{V2,}$ L_{V3} and eccentric distance of load e_z will be taken from the Cad model generated for spindle and bracket with taking reference from the figure:4.4 and the various loads on the bolt will be calculated using the relationship 3.33 to 3.37. The safe diameter of bolt will be calculated considering the factor of safety 6 and from the relationship 3.38 and 3.39

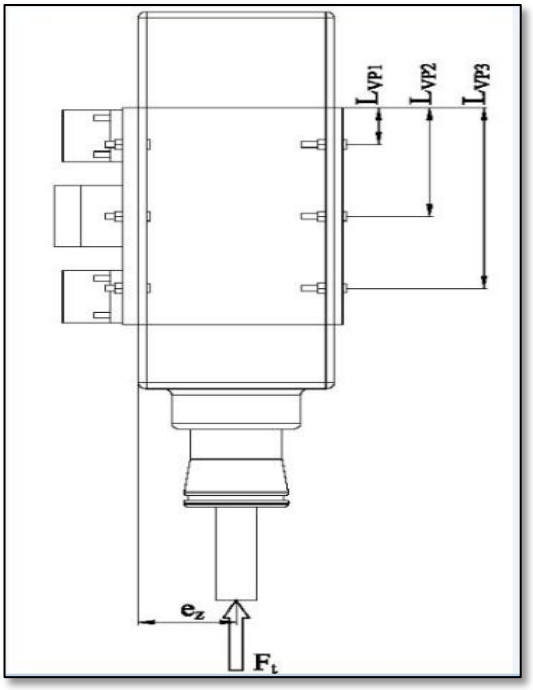

Figure 4.4: Distances of bolt from tilting edge when cutting along Z-axis

Table 4.10: Value for bolt diameter for cutting along Z-axis

Parameter	Symbol	Value	Unit
Load on clamping bolts in plunge cutting	W_p	272.3170	N
Direct shear load on each bolts	W_{ds}	45.3862	N
Eccentricity of load	e_Z	0.060 m	m
Vertical distance of bolts in first row from twisting edge	L_{v1}	0.0300	m
Vertical distance of bolts in second row from twisting edge	L_{v2}	0.0889	m
Vertical distance of bolts in third row from twisting edge	L_{v3}	0.1478	m
Maximum tensile load on bolt	Wt	6.5662	N
Equivalent tensile Load	W_{te}	48.7879	N
Equivalent shear Load	W_{se}	45.5048	N
Diameter of the bracket clamping bolt in tension	d_{btz}	0.8	mm
Diameter of the bracket bolt according to shearing	d_{bsz}	1.1	mm

The safe diameter of bolt will be taken from the above four calculated diameter of the bolts from these three cases that is 2.2 mm. Although the bolt diameter is coming out to be 2.2 mm but considering the dynamic behavior of the machine tool components a safe diameter of 4 mm is selected from the standard size available in the market.

4.3.2. Thickness of the Bracket plate

The Thickness of the bracket plate will be optimized using the FEM analysis in ANSYS. The CAD model of bracket is shown in figure 4.5.The initial boundary condition to the bracket plate shown in figure 4.6 is fixed support to the plate to be attached at Z-axis shown by symbol A, standard Gravity earth for considering the self weight of the assembly shown by symbol C, a pretension value to the bolts which occurs while tightening the bolt into the hole whose value should be equal to the axial load which it has to bear while cutting and is calculated in table 4.8 shown by symbol D. Here our focus is to consider the deflection on the Bracket plate therefore instead of tool a remote force is being applied at the same distance and of same magnitude. The spindle is given rigid connection because of that ANSYS does not calculate any result on the spindle and also doesn't do its meshing but it will consider it as a inter connected body which helps to stop the deflection of other bodies, as Deflection is to be calculated particularly on the bracket plate only.

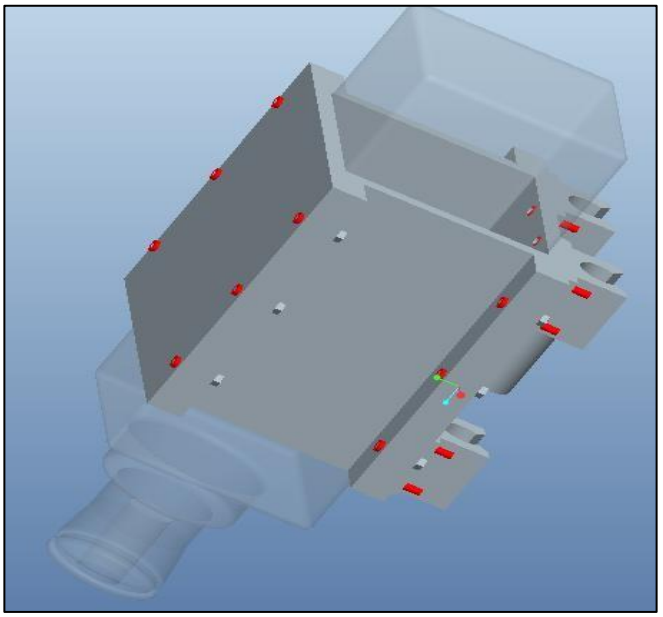

Figure 4.5: CAD model of the bracket plate

Material of the components is as shown in table:

Table 4.11: Material of components for analysis of bracket thicknesses

Component	Material
Bracket plate	Aluminum 6061O
Bolt	Stainless steel
Back plate	Structural steel

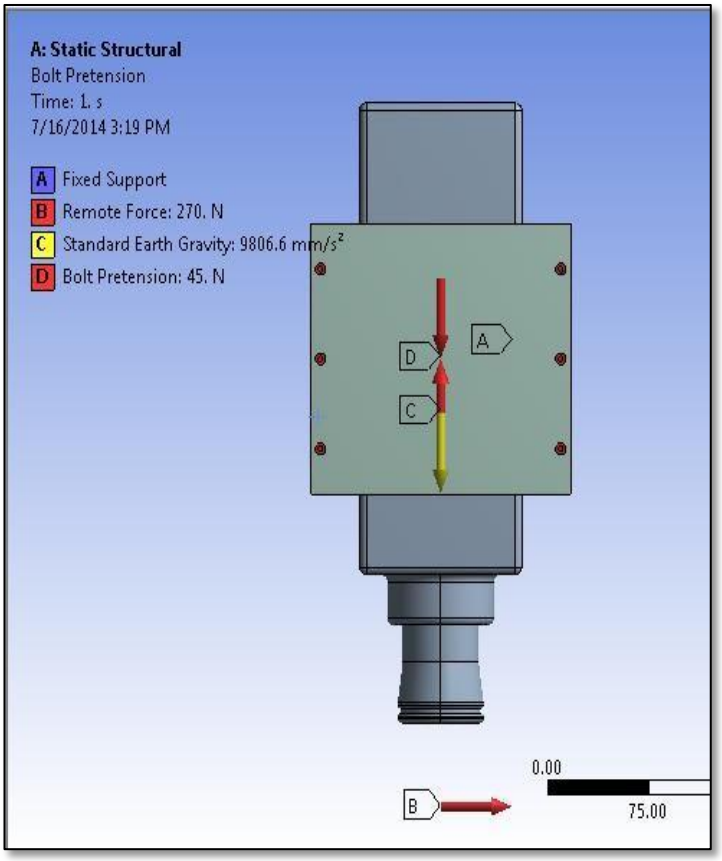

Figure 4.6: Initial boundary condition applied to bracket plate

The loads are tangential and plunge in nature applying in different orientation. The iteration for different loading conditions is required to observe the maximum deflection direction. The different loading orientation is given in figure 4.7.

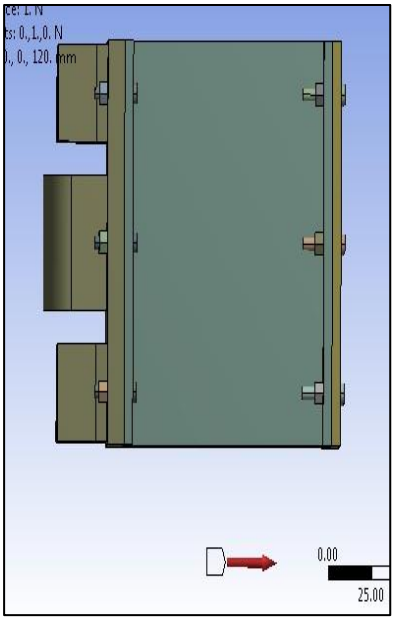

(a) Loading in positive X-direction

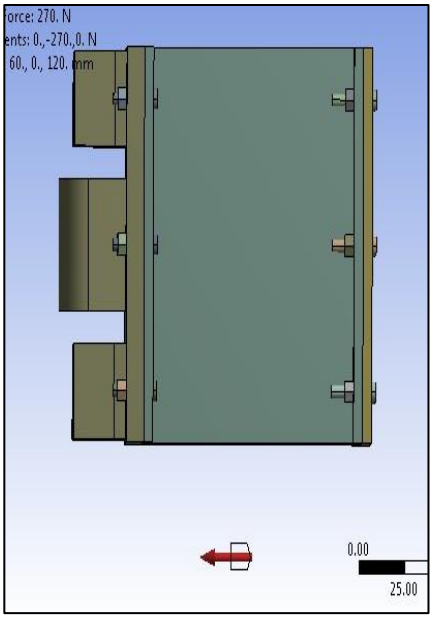

(b) loading in Negative X-direction

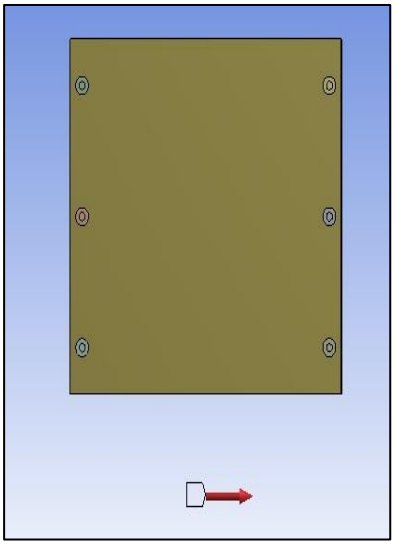

(c) Loading in positive Y-direction

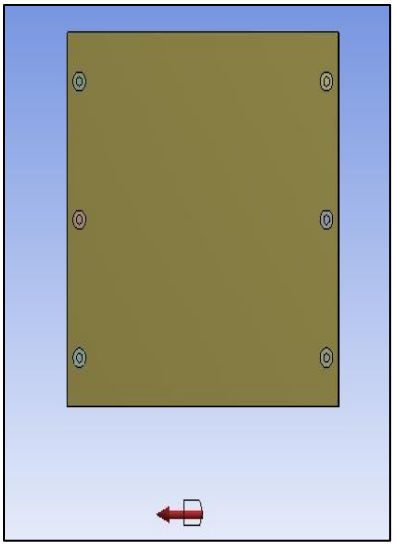

(d) loading in negative Y-direction

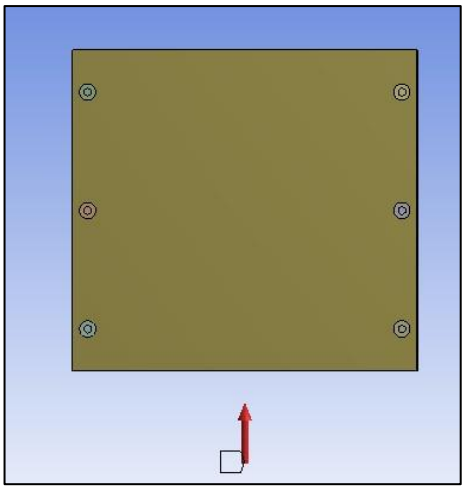

(e) Loading in Z direction

Figure 4.7: Loading in different orientation for bracket.

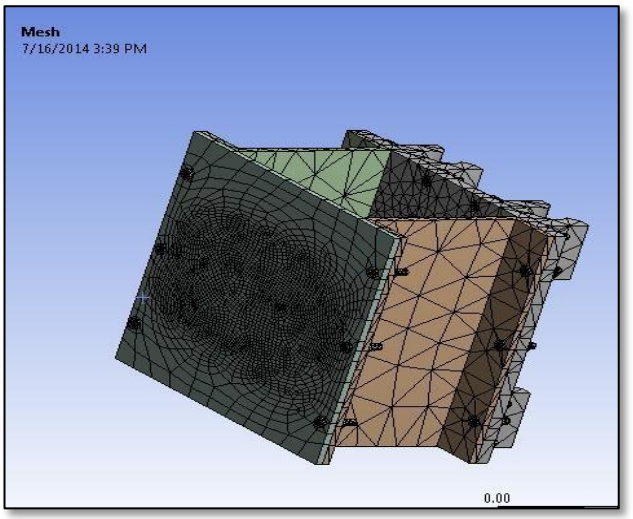

Figure 4.8: Mesh Generation in Bracket.

Triangular and tetrahedral mesh were generated with 66075 Nodes and 24696 elements as shown in figure 4.8

Table 4.12: Deflection and stress value for various bracket thicknesses

Bracket plate thickness : 8 mm			
Direction of Force	**Magnitude of force**	**Deflection**	**Von-mises Stress**
Positive X	270 N	0.0002535 mm	0.5312 Mpa
Negative X	270 N	0.0002535 mm	0.5312 Mpa
Positive Y	270 N	0.0002053 mm	0.4589 Mpa
Negative Y	270 N	0.0002053 mm	0.4589 Mpa
Z-direction	269 N	0.0000462 mm	0.28171 Mpa
Bracket plate thickness : 5 mm			
Direction of Force	**Magnitude of force**	**Deflection**	**Von-mises Stress**
Positive X	270 N	0.001623 mm	1.8673 Mpa
Negative X	270 N	0.001719 mm	1.8579 Mpa
Positive Y	270 N	0.001699 mm	1.6154 Mpa
Negative Y	270 N	0.001699 mm	1.6240 Mpa
Z-direction	269 N	0.000057 mm	0.3860 Mpa

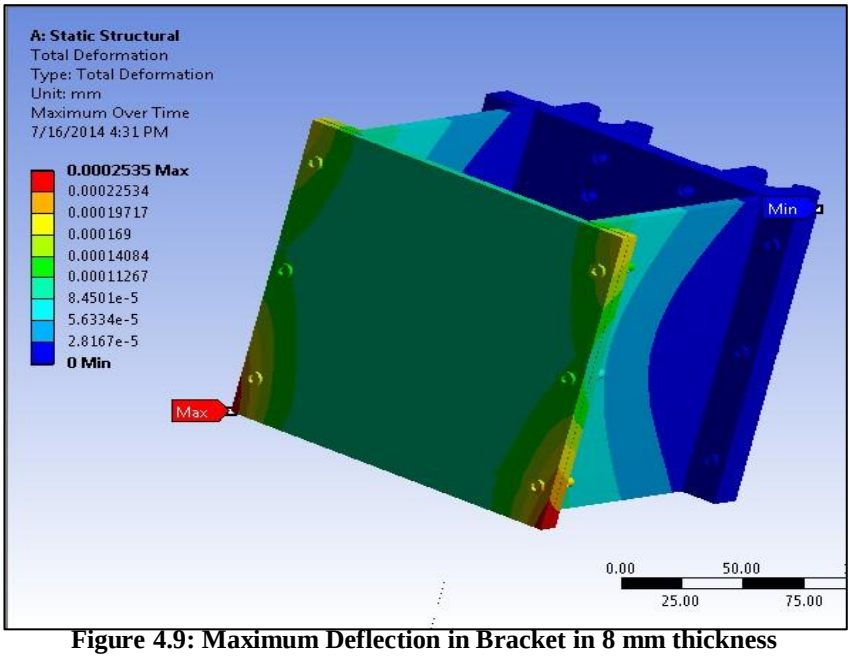

Figure 4.9: Maximum Deflection in Bracket in 8 mm thickness

From the iteration it was observed that a bracket thickness of 8 mm is very much safe in terms of deflection because all the deflections under all forces are below 1 micron as shown in figure4.9, so bracket thickness can be reduce. In the next iteration for a bracket thickness 5 mm the total deflection with subassembly 1 was reaching 1micron shown by figure 4.10 so a thickness of 5 mm was selected. Beyond which the thickness will reduce less than bolt diameter which is not allowed.

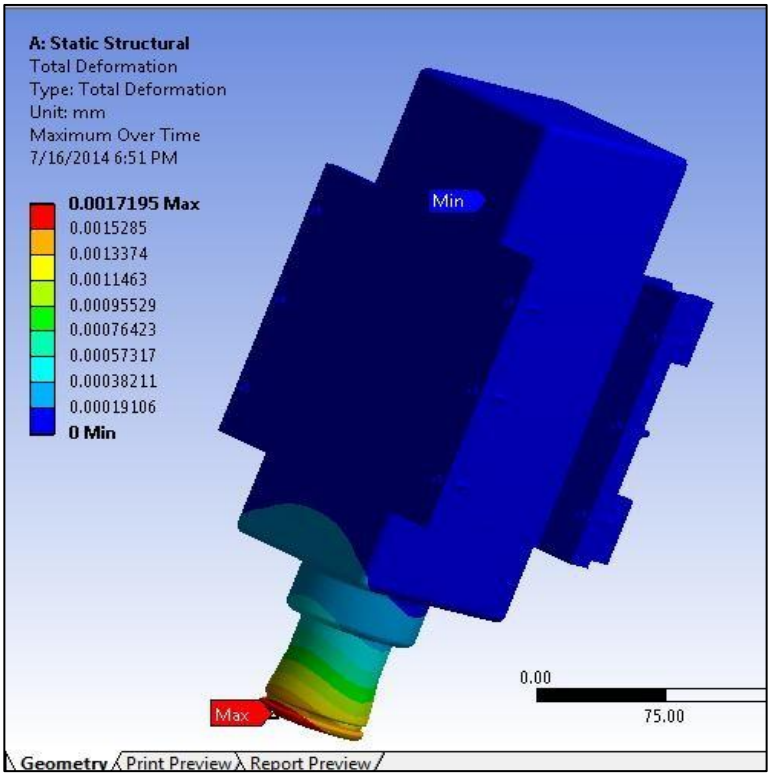

Figure 4.10: Maximum Deflection for 5 mm Bracket thickness

Check against the Tearing of the plate

The plate thickness should be checked against the tearing done by the hole created for the bolts. From the equation 3.40 and the selected diameter of the bolt and thickness of the bracket plate the bearing stress is being calculated in the table 4.13 given below

Table 4.13: Bearing stress calculation in bracket plate

Parameter	Symbol	Value	Unit
Thickness of the bracket plate	B_t	5	mm
Bolt diameter	d_b	4	mm

Maximum force from tangential and plunge cutting	F_m	270	N
Calculated value of the bearing stress	$\sigma_{bcalculated}$	13.5	Mpa

The calculated bearing stress is coming through 13.5 Mpa and the allowable bearing stress for bracket material is 228 Mpa. Therefore the thickness of the bracket is safe against the tearing.

4.4. Z-AXIS DRIVE SELECTION

The Z-axis drive is composed of the components such as ball screw, drive motor, coupling which are mounted on the slide way. Apart from that it is also supporting the spindle and bracket arrangement. The selection will be done on the basis of empirical relationship discussed in chapter 3.

4.4.1 Selection of ball screw.

Ball screw selection is based upon the parameters selected for the drive motor which runs the ball screw to transmit the motion.

Table 4.14: Drive motor parameter

Parameter	**Value**	**Unit**
Minimum delay between two steps (commands)	5	ms
step angle	1.8	degree
steps required per rotation	200.0000	
rotations per minute	60.0000	rpm

The calculation for the ball screw is done using the empirical relationship as discussed in the previous chapter. The material of ball screw is taken as Chrome steel which is suitable material under both type of loading i.e. axial and Torsional and its properties are as follows

Table 4.15: Mechanical properties of the Chrome Steel [39]

Density	7833 Kg/m^3
Young's Modulus	234 GPa
Poisson's ratio	0.29
Ultimate tensile strength	2650 MPa
Ultimate Yield Strength	2070 Mpa

Ball screw at same time is under two different type of loading i.e. is axial and Torsional, therefore Von-Mises stress criteria is used to determine the diameter of the ball screw. The permissible Von-Mises stress value for the material is 147 Mpa[37] with a factor of safety taken as 7 for machine tool with Vibration and impact[40].The equation 3.41 to equation 3.61 were used to calculate the ball screw diameter as shown in table 4.16

Table 4.16: calculation for the value of the ball screw diameter for Z-axis

Parameter	Symbol	Value	Unit
Lead of screw	l_Z	0.0050	m
Maximum Linear Speed	S_Z	0.0050	m/sec
Motor's rated rotational speed	N_{mZ}	60	rpm
Acceleration time	t_{accZ}	0.1500	sec
Acceleration	α_Z	0.0333	m/sce^2
Friction coefficient of round shaft	μR	0.1250	
Guide surface resistance	F_{frZ}	108.4319	N
Axial load During forward acceleration	F_{az1}	255.4223	N
Axial load During forward uniform motion	F_{az2}	254.0373	N
Axial load During forward deceleration	F_{az3}	252.6524	N
Axial load During backward acceleration	F_{az4}	305.6635	N
Axial load During uniform backward motion	F_{az5}	307.0485	N
Axial load During backward deceleration	F_{az6}	308.4334	N
Maximum axial load applied on the Ball Screw	F_{azmax}	308.4334	N
Sliding screw efficiency	η_{sc}	0.8500	
Driving torque to obtain thrust force	T_{tz}	0.2889	N-m
Diameter according to maximum allowable stress	d_{bscz}	0.0100 m	m
Maximum permissible von mises stress	σ_{max}	4683924.0459	N/m^2
Standard diameter available in round shaft model	d_{bavz}	0.0160	m
length of feed screw	L_{fz}	0.3100	m

4.4.2 Selection of sideway.

As the selection of the slide way for Z- direction depends upon the bending moment, from the figure 3.8, figure 3.9 and figure 3.10 we will calculate a rough dimension choosing the smallest model and creating its CAD model as shown in figure 4.11.

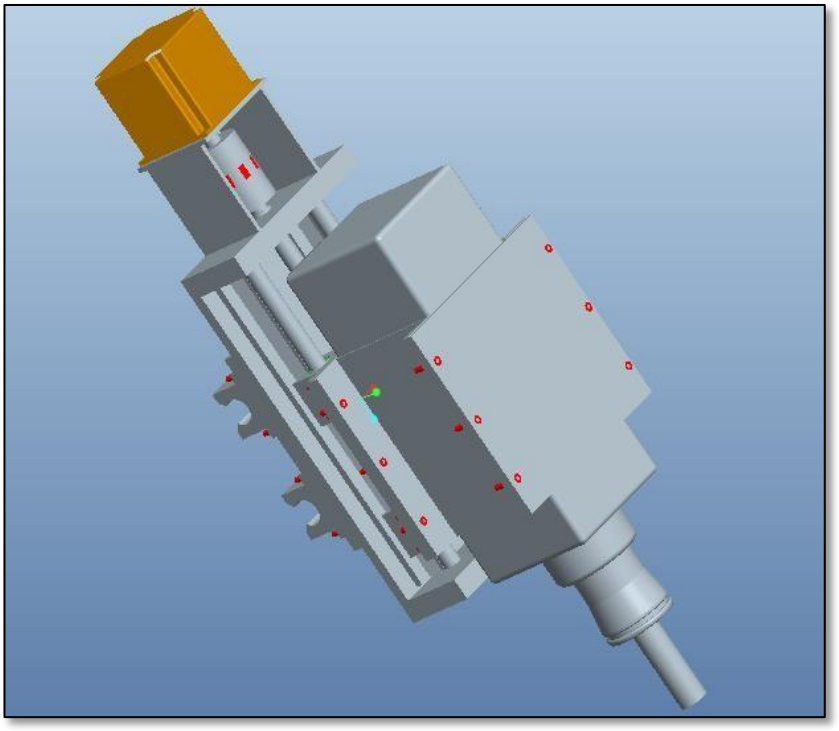

Figure 4.11: CAD model of Z-axis Drive

Further bending moments in X axis is calculated from the equation 3.62 and in the Y-axis is calculated from equation 3.63 and 3.64.

Table 4.17: Bending moment in z-axis slide

For Tangential cutting force	
a) when cutting in X-axis	
Distance between cutting force and farthest bearing block along Z	0.3803 m
Maximum Bending Moment in Y axis due to tangential force	102.9572 N-m
b) when cutting in Y-axis	
Distance between cutting force and center of back plate along Z	0.3140 m
Maximum Bending Moment in x axis due to tangential force	85.0000 N-m
For plunge cutting force(in z axis)	
Distance between plunging force and center of bearing along X	0.0960 m
Maximum Bending Moment in Y axis due to plunge force	8.9371 N-m

The permissible range of bending moments according to manufacturer of the round shaft in Z-axis is given below in the table from which the safe model will be selected.

Table 4.18: Diameter of round shaft available against the bending moment in Z-axis drive

Diameter of round shaft rod(mm)	F_{max}(N)	M_x(N-m)	M_y(N-m)
12.7	1157	163	169
15.875	1334	311	311
19.05	1334	325	325
25.4	2669	565	501
31.75	3003	1073	989
38.1	3158	1627	1424
50.8	4003	3649	3169

Therefore shaft diameter of 12.7mm is chosen from the above table

4.4.3 Selection of driving motor

The Drive motor selected for the Z-axis drive is calculated from the equation 3.68 to equation 3.74. For the Z-axis drive motor Gravity Torque is considered because the motor has to work against the gravity in Z-axis drive motor.

Table 4.19: Motor torque calculation for Z-axis drive motor

Parameter	Symbol	Value	Unit
Inertia of pinion	J_{z1}	0.0000	
Inertia of gear	J_{z2}	0.0000	
Inertia of feed screw	J_{z3}	0.00001562	kg-m^2
Inertia of work and table	J_{z4}	0.0010	kg-m^2
Number of pinion teeth	$N1$	0.0000	
Number of gear teeth	$N2$	0.0000	
Step angle per pulse	θ	1.8000	degree
Pitch of feed screw in rev/mm	P_{revz}	0.2000	
Density of feed screw material	ρ	7833.0000	kg/m^3
Radius of feed screw rod	r_{bz}	0.0080	m
Length of feed screw	L_{fz}	0.3100	m
Angular Accereleration	α_{az}	6.6000	rad/sec^2
Transmission efficiency	e	0.8000	
Co-efficient of friction	μ	0.1250	
Gravity torque	T_{gz}	0.4155	N-m
Friction torque	T_{fz}	0.0507	N-m

Thrust Torque	T_{tz}	0.2889	N-m
Acceleration torque	$T_{\alpha z}$	0.0087	N/m^2
Total Torque	T_{total}	0.7638	N-m

The standard available torque near to the calculated peak torque of 0.7638 N-m is of NEMA 23 model M1233021 having a value of holding torque of 0.8 N-m.

4.4.4 Selection of the Coupling

The coupling for ball screw and Z-axis drive motor is calculated from the equation 3.75 to equation 3.80

Table 4.20: calculation for Coupling in Z-axis

Parameter	Symbol	Value	Unit
Temperature Effect	S_t	1.2	
Torsional stiffness Factor	S_d	5	
Operating Factor	S_A	1.8	
Rotational inertia coefficient of load side	m_{Alz}	0.883000003	
Moment of inertia of driving side	J_{az}	0.000145	$kg\text{-}m^2$
Moment of inertia of load side	J_{lz}	0.001094316	$kg\text{-}m^2$
Moment of inertia of Coupling	J_{kz}	0.00008	$kg\text{-}m^2$
Moment of inertia of Motor	J_{motz}	0.000105	$kg\text{-}m^2$
Moment of inertia of ball screw	J_{bsz}	0.00001562	$kg\text{-}m^2$
Moment of inertia of slide and work piece	J_{schlz}	0.001038701	$kg\text{-}m^2$
Maximum Driving torque	T_{ASz}	0.2889	N-m
Peak torque	T_{pcz}	0.459183281	N-m
Rated torque of the coupling	T_{KNz}	2.755099689	N-m

The selection of coupling is based upon the rated torque according to the standard available couplings, The Standard available rated torque coupling available is of 5 N-m above the calculated 2.75 N-m so it has been selected.

4.5 ANALYSIS OF Z-AXIS DRIVE

According to the calculation model having shaft diameter12.7 mm is suitable for this range of bending moments. Analysis is done in ANSYS by creating the FEM model of the Z-axis Drive as shown in figure 4.12.

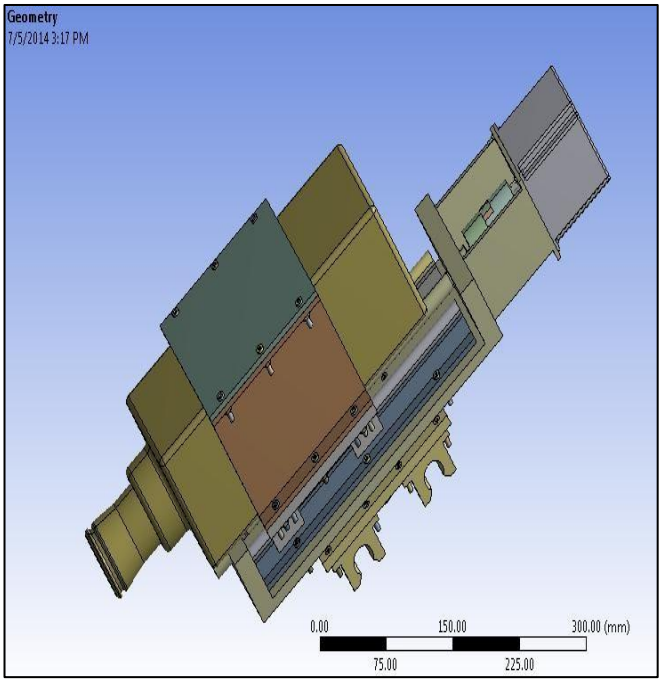

Figure 4.12: Z-axis Drive

The materials of the components of the Z-axis drives are:

Table 4.21: Material of components for analysis of Z-axis

Component	**Material**
Bracket plate	Aluminum 6061O
Bolt	Stainless steel
Back plate	Structural steel
Spindle	Structural steel
Coupling	Polyurethane
Ball screw	Chrome steel
Round shaft	Stainless steel
Supporting rail of shaft	Aluminum 6061O
Slide base plate	Structural steel

The initial boundary conditions are giving fixed support to the back plate which will attach ay Y-axis shown with symbol A , standard gravity earth to consider the self weight of the assembly shown with the symbol C and force in the various directions as shown with symbol B as shown in the figure 4.13. Mesh is generated having triangular and tetrahedral shape with 131410 nodes and 60212 elements shown in figure 4.14

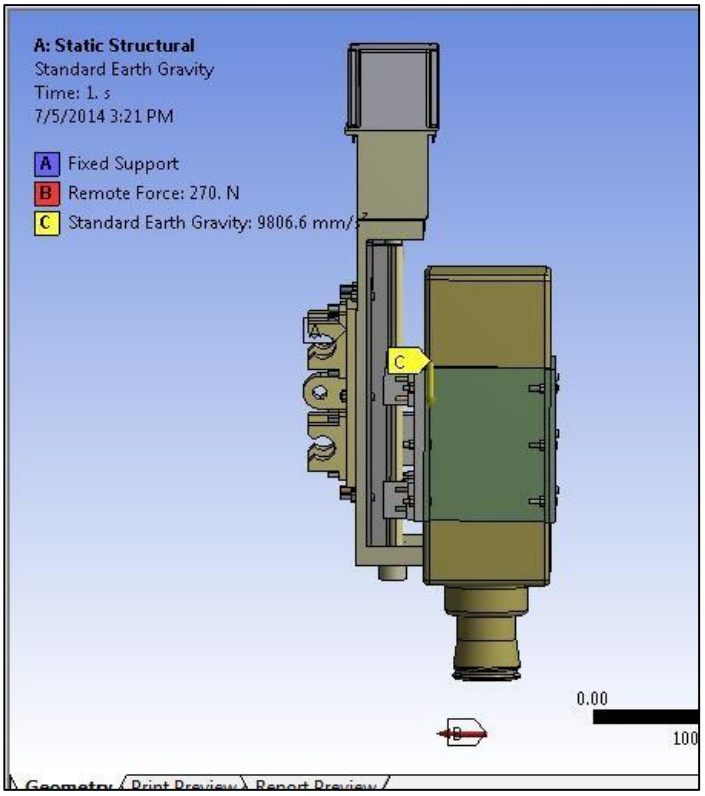

Figure 4.13: Z-axis Drive with boundary conditions

.

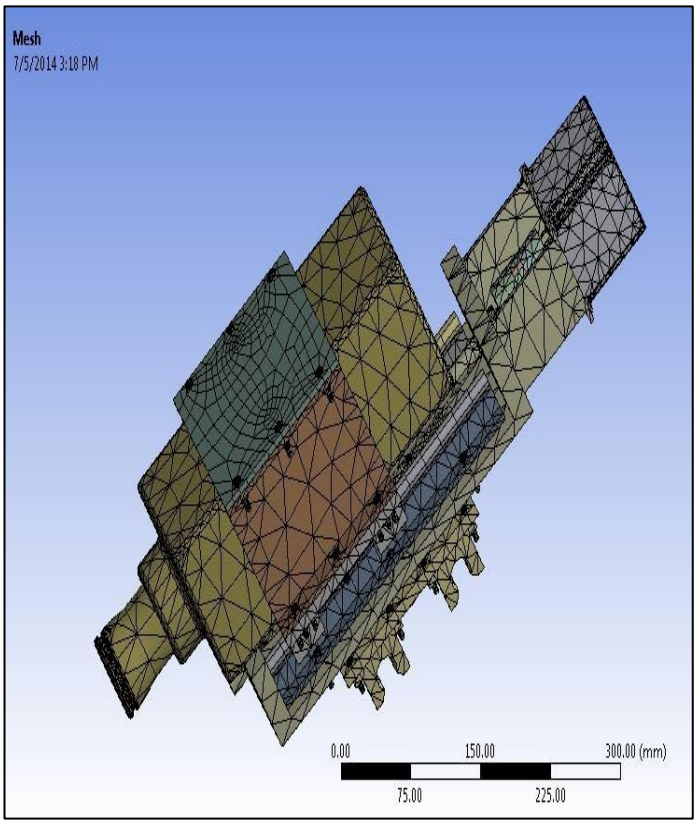

Figure 4.14: Mesh structure of Z-axis Drive

The different loading conditions are shown in figure 4.15.

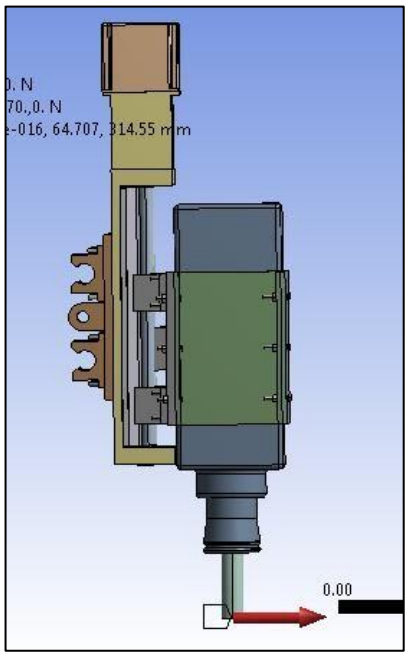

(a) Loading in positive X-direction

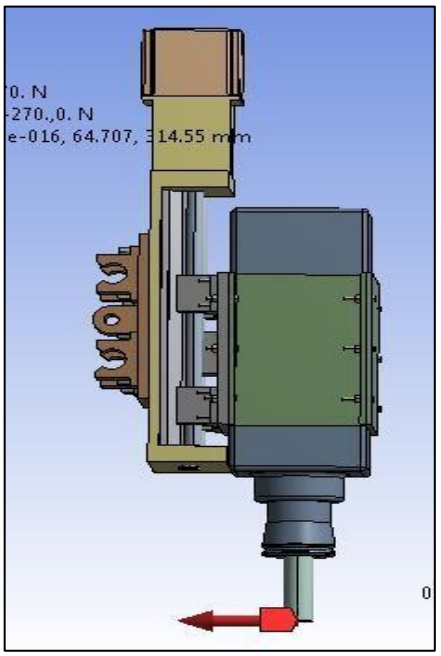

(b) loading in Negative X-direction

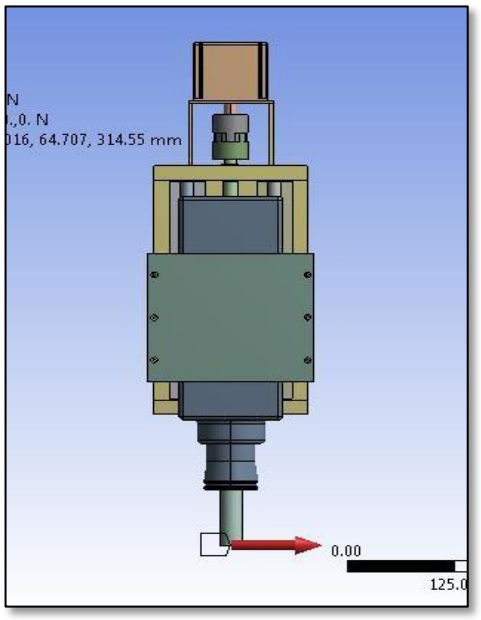

(c) Loading in positive Y-direction

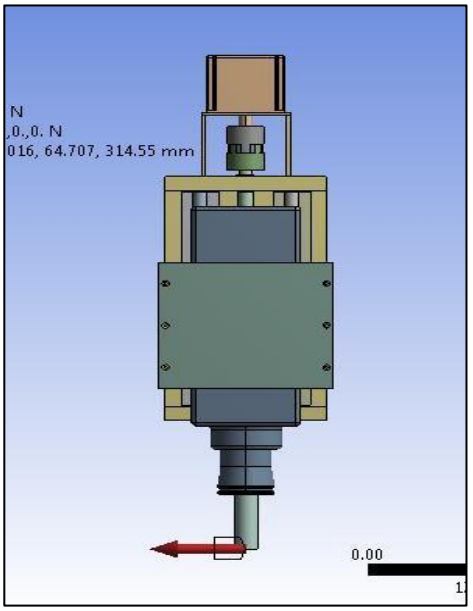

(d) loading in negative Y-direction

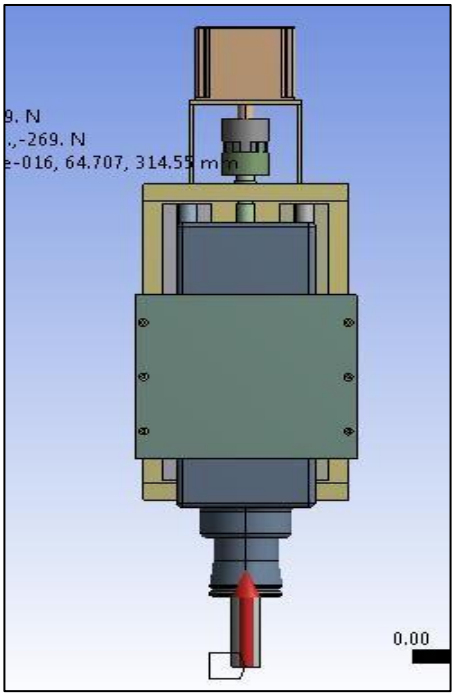

(e) Loading in Z direction

Figure 4.15: Loading direction in different orientation for Z-axis

The iteration is also found out in all these directions as shown below:

Table 4.22: Iteration result for the deflection in Z-axis drive

Round shaft diameter 12.7 mm			
Direction of Force	**Magnitude of force**	**Deflection**	**Von-mises Stress**
Positive X	270 N	0.00490 mm	6.5254 Mpa
Negative X	270 N	0.00252 mm	1.8426 Mpa
Positive Y	270 N	0.00350 mm	4.9855 Mpa
Negative Y	270 N	0.00349 mm	4.9710 Mpa
Z-direction	269 N	0.00266 mm	0.8741 Mpa
Round shaft diameter 15.875 mm			
Direction of Force	**Magnitude of force**	**Deflection**	**Von-mises Stress**
Positive X	270 N	0.00320 mm	3.5217 Mpa
Negative X	270 N	0.00194 mm	1.8688 Mpa
Positive Y	270 N	0.00271 mm	2.7638 Mpa
Negative Y	270 N	0.00272 mm	2.7632 Mpa
Z-direction	269 N	0.00171 mm	0.5382 Mpa

From the iteration it is observed that the model selected numerically has deflection upto 5 micron shown by figure 4.16 and can be reduced by selecting hire model, in which the deflection is maximum at positive X axis which is below 3.5 micron and other direction deflections are also within 1 to 2 micron shown in figure 4.17. Selection of further hire model can add towards cost and increase in self weigth of the assembly. Therefore rod diameter 15.875 mm is selected for Z-axis drive.

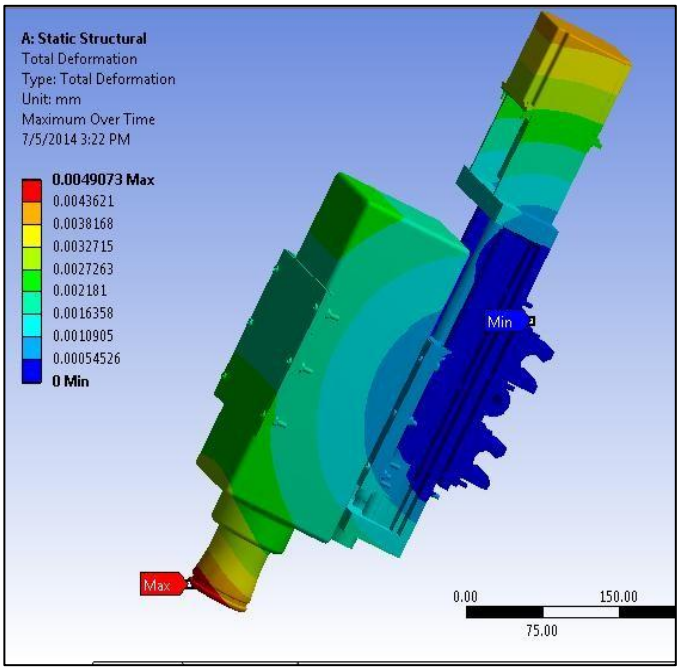

Figure 4.16: Maximum Deformation in Z-axis Drive for 12.7 mm diameter

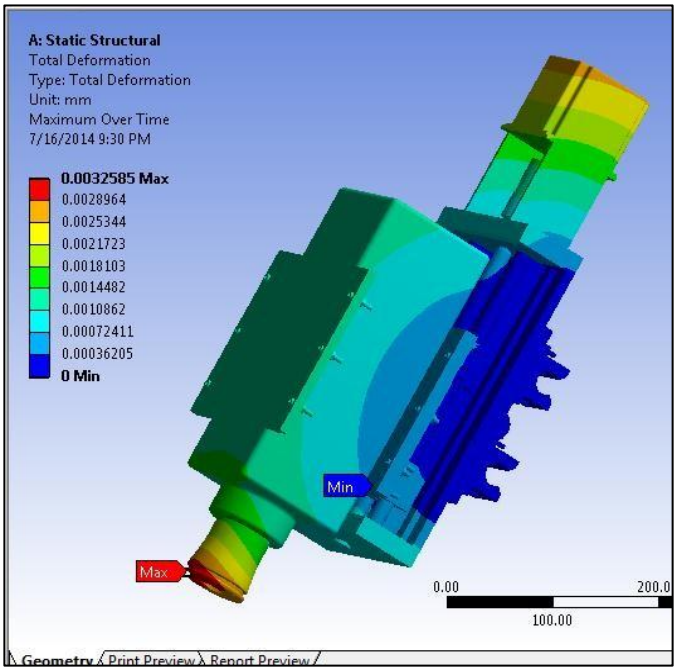

Figure 4.17: Maximum deformation in Z-axis Drive with diameter 15.875

4.6 Y-AXIS DRIVE SELECTION

The Y-axis drive selection will be carried out same as that for Z –axis but the drive length of the Y – axis is very large as compare to Z and it is also supporting the Z-axis assembly. Therefore components selection will be having hire rating of that of Z-axis.

4.6.1 Selection of ball screw.

The procedure for selection of ball screw is same as in the case of Z-axis

Table 4.23: Ball screw calculation for Y-axis drive

Parameter	**Symbol**	**Value**	**Unit**
Lead of screw	L_Y	0.0125	m
Maximum Linear Speed	S_Y	0.0125	m/sec
Motor's rated rotational speed	N_{my}	60	rpm
Acceleration time	t_{accy}	0.1500	sec
Acceleration	α_y	0.0833	m/sce^2
Friction coefficient of round shaft	μR	0.1250	
Guide surface resistance	F_{fry}	341.1838	N
Axial load During forward acceleration	F_{ay1}	1240.8539	N
Axial load During forward uniform motion	F_{ay2}	1235.6558	N
Axial load During forward deceleration	F_{ay3}	1230.4577	N
Axial load During backward acceleration	F_{ay4}	305.6635	N
Axial load During uniform backward motion	F_{ay5}	307.0485	N
Axial load During backward deceleration	F_{ay6}	308.4334	N
Maximum axial load applied on the Ball Screw	F_{aymax}	1240.8539	N
Sliding screw efficiency	η_{sc}	0.8500	
Driving torque to obtain thrust force	T_{ty}	2.9057	N-m
Diameter according to maximum allowable stress	d_{bscy}	0.0140 m	m
Maximum permissible von mises stress	σ_{max}	12344487.5371	N/m^2
Standard diameter available in round shaft 08 model	d_{bavy}	0.0250	m
length of feed screw	L_{fy}	2.3200	m

4.6.2 Selection of slide way.

As the selection of the slide way for Y- direction depends upon the bending moment, from the figure 3.12, figure 3.13 and figure 3.14 we will calculate a rough dimension choosing the smallest CAD model as shown in figure 4.18.

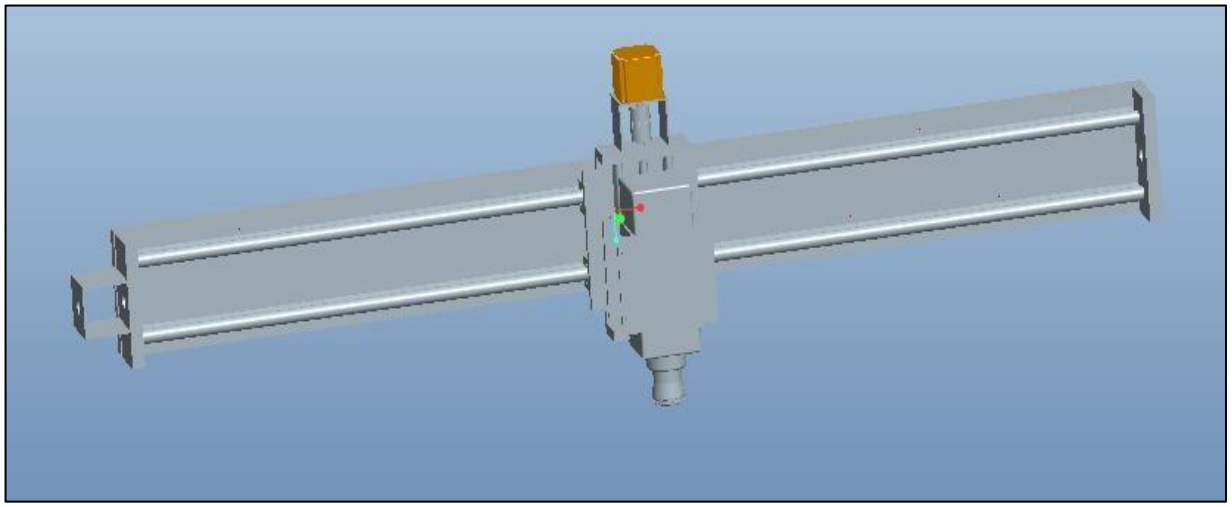

Figure 4.18: CAD model of Y-axis Drive

Further bending moments in X axis is calculated from the equation 3.65 and in the Y-axis is calculated from equation 3.66 and 3.67.

Table 4.24: Bending moment in Y-axis slide

For Tangential cutting force	
a) when cutting in X-axis	
Distance between cutting force and farthest bearing block along Z	0.4010 m
Maximum Bending Moment in Y axis due to tangential force	108.5510 N-m
b) when cutting in Y-axis	
Distance between cutting force and center of back plate along Z	0.3312 m
Maximum Bending Moment in x axis due to tangential force	89.6636 N-m
For plunge cutting force(in z axis)	
Distance between plunging force and center of bearing along X	0.1727 m
Maximum Bending Moment in Y axis due to plunge force	43.1676 N-m

The permissible range of bending moments according to manufacturer of the round shaft in Y-axis is given below in the table

Table 4.25: Permissible value of bending moments for Y-axis drive

Diameter of round shaft rod(mm)	F_{max}(N)	M_x(N-m)	M_y(N-m)
12.7	2402	103	169
15.875	3381	190	311
19.05	3737	193	325
25.4	4671	373	501
31.75	7784	698	989
38.1	9341	1085	1424
50.8	14679	2147	3169

Therefore round shaft diameter 12.7 mm is coming out to be safe model but diameter 19.05mm will be chosen from the above table because the Y-axis drive has to support Z- axis drive having rod diameter 15.875 and length of Y-axis is very large to stand against deflection.

4.6.3 Selection of driving motor

The driving torque in Y-axis will not be influenced with the gravity torque. The Drive motor selected for the Y-axis drive is calculated from the equation 3.68 to equation 3.74.

Table 4.26: Y-axis drive motor calculation

Parameter	Symbol	Value	Unit
Inertia of pinion	J_{y1}	0.0000	
Inertia of gear	J_{y2}	0.0000	
Inertia of feed screw	J_{y3}	0.01114489	kg-m^2
Inertia of work and table	J_{y4}	0.0097	kg-m^2
Number of pinion teeth	*N1*	0.0000	
Number of gear teeth	*N2*	0.0000	
Step angle per pulse	Θ	1.8000	degree
Pitch of feed screw in rev/mm	P_{revy}	0.0800	
Density of feed screw material	*P*	7833.0000	kg/m^3
Radius of feed screw rod	r_{by}	0.0125	m
Length of feed screw	L_{fy}	2.3200	m
Angular Accereleration	α_{ay}	6.6000	rad/sec^2
Transmission efficiency	*e*	0.8000	
Co-efficient of friction	μ	0.1250	

Gravity torque	T_{gy}	1.5594	N-m
Friction torque	T_{fy}	0.0194	N-m
Thrust Torque	T_{ty}	2.9057	N-m
Acceleration torque	$T_{\alpha y}$	0.1724	N/m^2
Total Torque	T_{total}	3.0975	N-m

The standard available torque near to the calculated peak torque of 3.0975 N-m is of NEMA 34 model M1343011 having a value of holding torque of 3.1 N-m

4.6.4 Selection of the Coupling

The coupling for ball screw and Y-axis drive motor is calculated from the equation 3.75 to equation 3.80

Table 4.27: coupling calculation for Y-axis drive

Parameter	**Symbol**	**Value**	**Unit**
Temperature Effect	S_t	1.2	
Torsional stiffness Factor	S_d	3	
Operating Factor	S_A	1.8	
Rotational inertia coefficient of load side	m_{Aly}	0.989598757	
Moment of inertia of driving side	J_{ay}	0.00022	$kg\text{-}m^2$
Moment of inertia of load side	J_{ly}	0.020931318	$kg\text{-}m^2$
Moment of inertia of Coupling	J_{ky}	0.00008	$kg\text{-}m^2$
Moment of inertia of Motor	J_{moty}	0.00018	$kg\text{-}m^2$
Moment of inertia of ball screw	J_{bsy}	0.00001562	$kg\text{-}m^2$
Moment of inertia of slide and work piece	J_{schly}	0.009746428	$kg\text{-}m^2$
Maximum Driving torque	T_{ASy}	2.9057	N-m
Peak torque	T_{pcy}	5.175874677	N-m
Rated torque of the coupling	T_{KNy}	18.63314884	N-m

The standard rated torque coupling available near to calculated value is of 21 N-m.

4.7 ANALYSIS OF Y-AXIS DRIVE

Analysis is done in ANSYS by creating the FEM model of the Y-axis Drive. The CAD model can be seen in figure 4.19. The Boundary condition applied shown in figure 4.20 are giving

fixed support to the both ends of the Y-axis drive as shown by symbol C, standard gravity earth is given to consider the self weight of the assembly shown by Symbol B and remote force is shown by the symbol A.

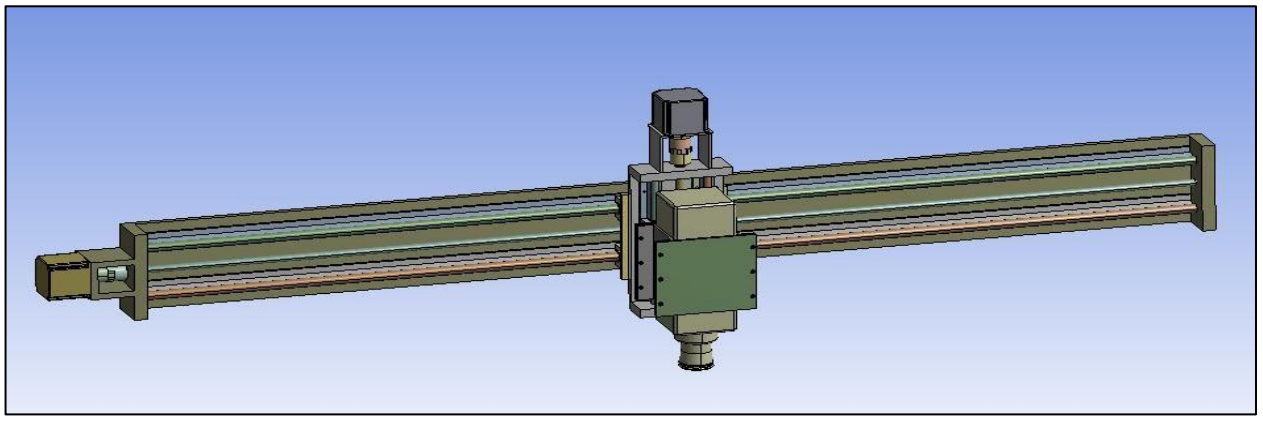

Figure 4.19: Y-axis Drive

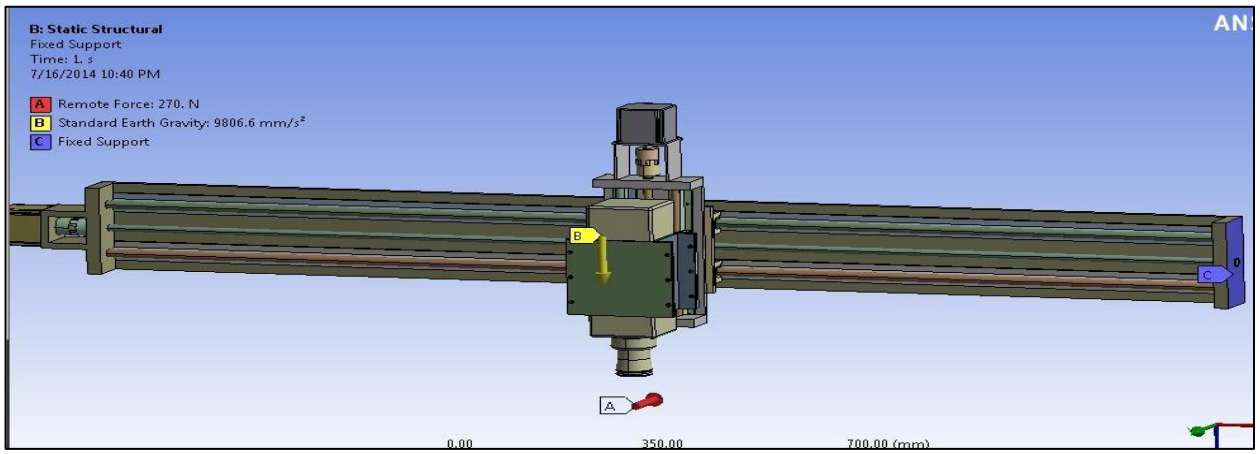

Figure 4.20: Y-axis Drive with boundary conditions

The materials of the components of the Y-axis drives are:

Table 4.28: Material of components for analysis of Y-axis

Component	Material
Bracket plate	Aluminum 6061O
Bolt	Stainless steel
Back plate	Structural steel
Spindle	Structural steel
Coupling	Polyurethane
Ball screw of Z-axis and Y-axis	Chrome steel
Round shaft of Z-axis and Y-axis	Stainless steel
Supporting rail of shaft of Z-axis and Y-axis	Aluminum 6061O
Slide base plate of Z-axis and Y-axis	Structural steel

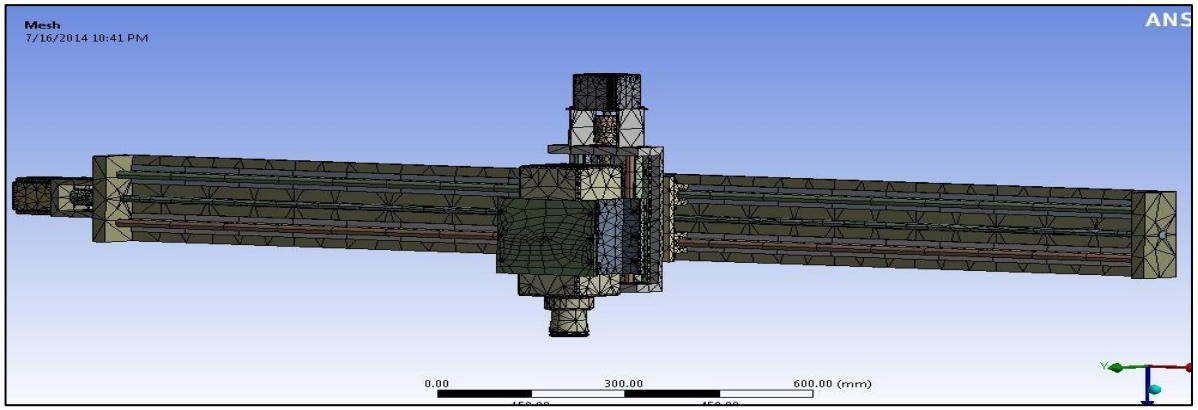

Figure 4.21: Mesh structure of Y-axis Drive

Mesh is generated with 41989 elements and 89596 nodes shown in figure 4.21.The different loading conditions are mention in the figure. The different loading conditions were required to observe the most influencing force direction which will cause maximum deflection. The different loading orientation is shown in fig 4.22

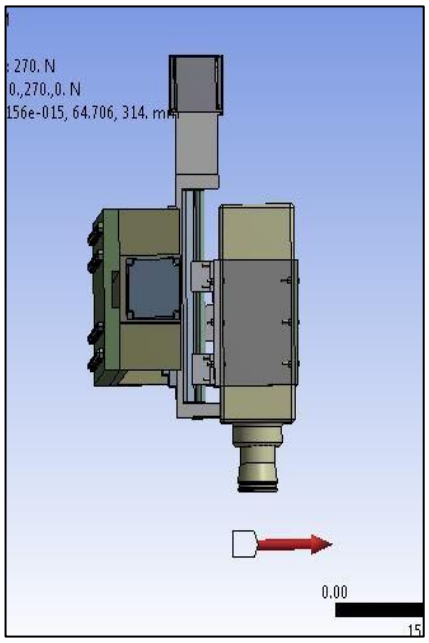

(a) Loading in positive X-direction

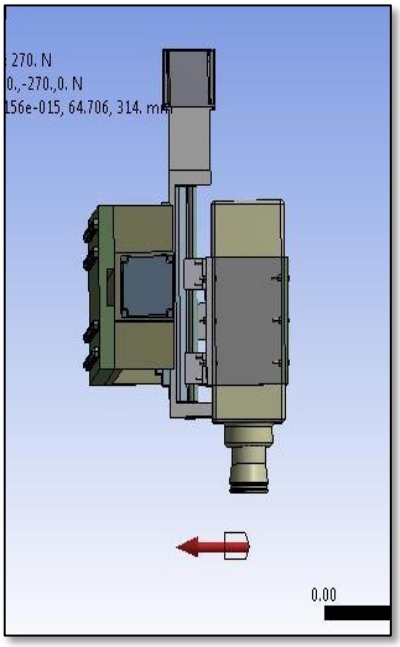

(b) Loading in Negative X-direction

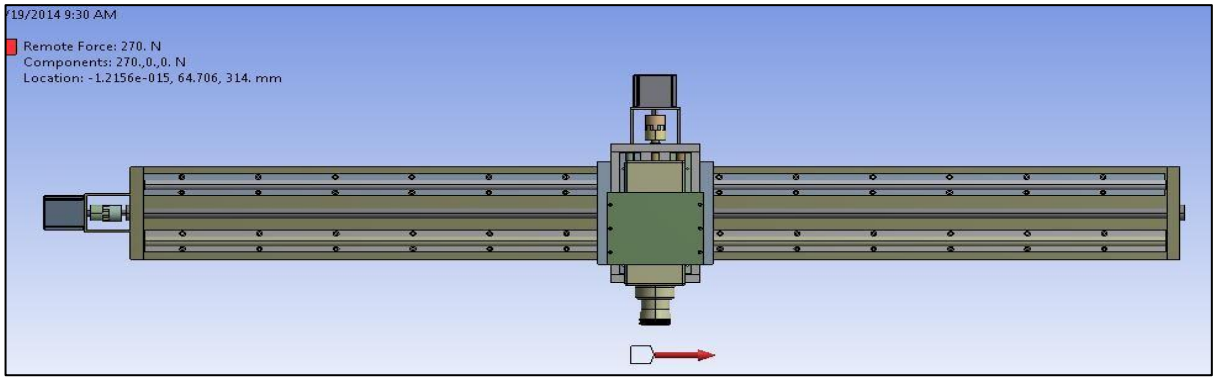

(c) Loading in positive Y-direction

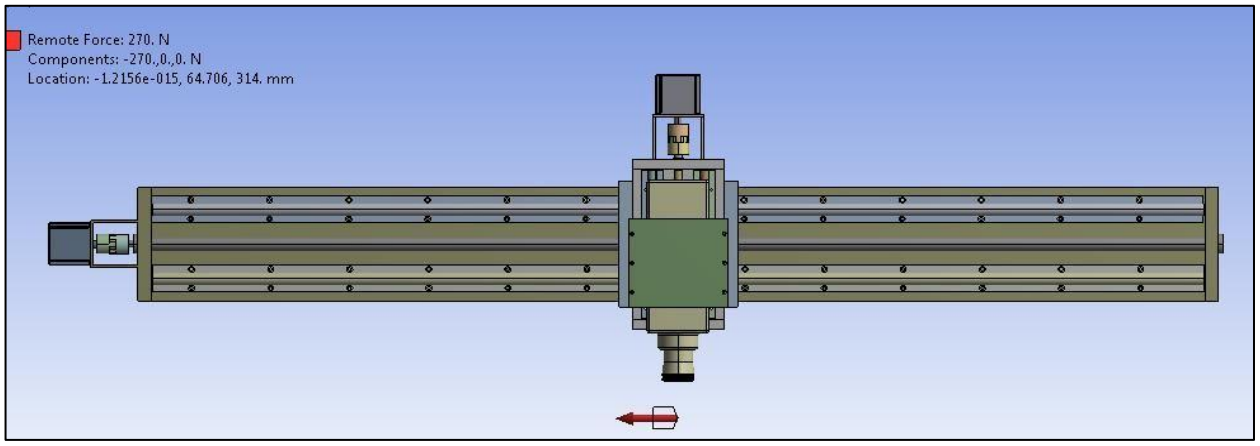

(d) Loading in negative Y-direction

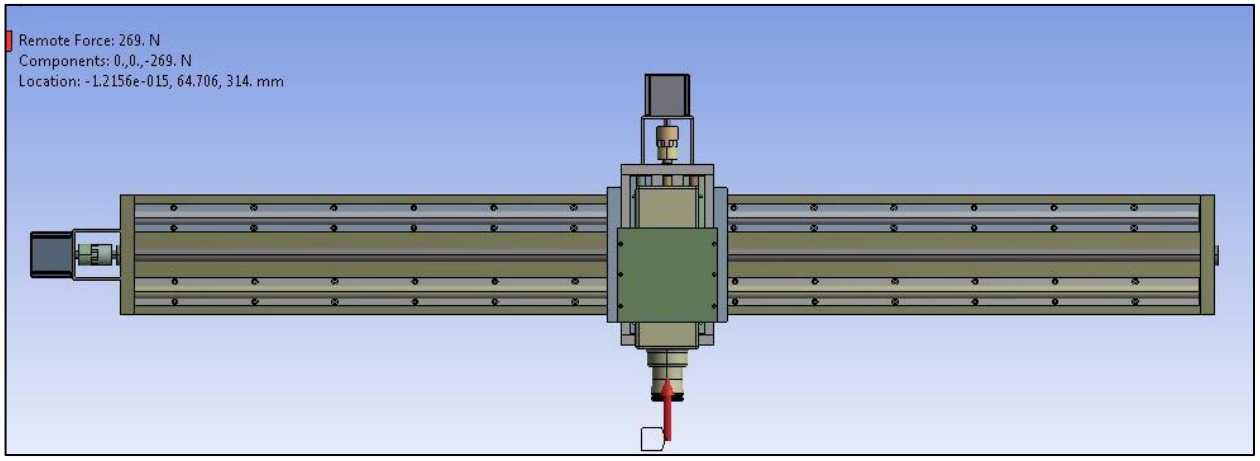

(e) Loading in Z direction

Figure 4.22: Loading direction in different orientation of Y-slide

Table 4.29: Iteration for deflection value in Y-axis slide

Round shaft with 19.05 mm diameter		
Direction of Force	**Deflection**	**Von-mises Stress**
Positive X	0.02538 mm	9.1536 Mpa
Negative X	0.00612 mm	2.1795 Mpa
Positive Y	0.01153 mm	4.8113 Mpa
Negative Y	0.01151 mm	5.1367 Mpa
Z-direction	0.00374 mm	2.0422 Mpa
Round shaft with 25.4 mm diameter		
Direction of Force	**Deflection**	**Von-mises Stress**
Positive X	0.01042 mm	4.0283 Mpa
Negative X	0.00412 mm	2.2150 Mpa

Positive Y	0.00538 mm	2.4629 Mpa
Negative Y	0.00535 mm	2.4294 Mpa
Z-direction	0.00123 mm	0.7484 Mpa
Round shaft with 25.4 mm diameter and back plate of Aluminum of thickness 25 mm		
Direction of Force	**Deflection**	**Von-mises Stress**
Positive X	0.00966 mm	3.8732 Mpa
Negative X	0.00443 mm	2.2150 Mpa
Positive Y	0.00495 mm	2.3961 Mpa
Negative Y	0.00491 mm	2.3720 Mpa
Z-direction	0.00091 mm	0.7483 Mpa

It has been observed with the iteration that with model having shaft diameter 19.05 mm deflection in the Y-axis axis drive has gone above 25 micron as shown in figure 4.23, so next iteration was done with model having diameter 25.4 mm and the deflection was still above 10 micron shown in figure 4.24. This deflection was due to the long length of Y-axis drive that is 2032 mm, with the use of Aluminum back plate bolted behind the same model having shaft diameter 25.4 mm shown in figure 4.25 deflection was gone under 10 micron as shown in figure 4.26. So the design was quite safe.

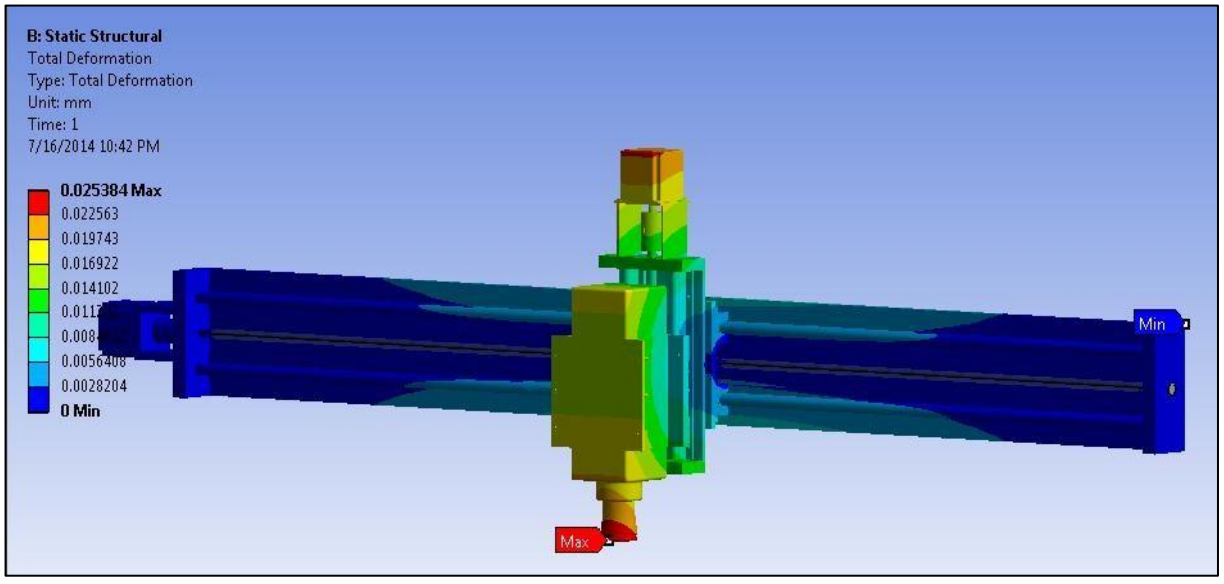

Figure 4.23: Maximum Deformation in Y-axis Drive with 19.05mm shaft

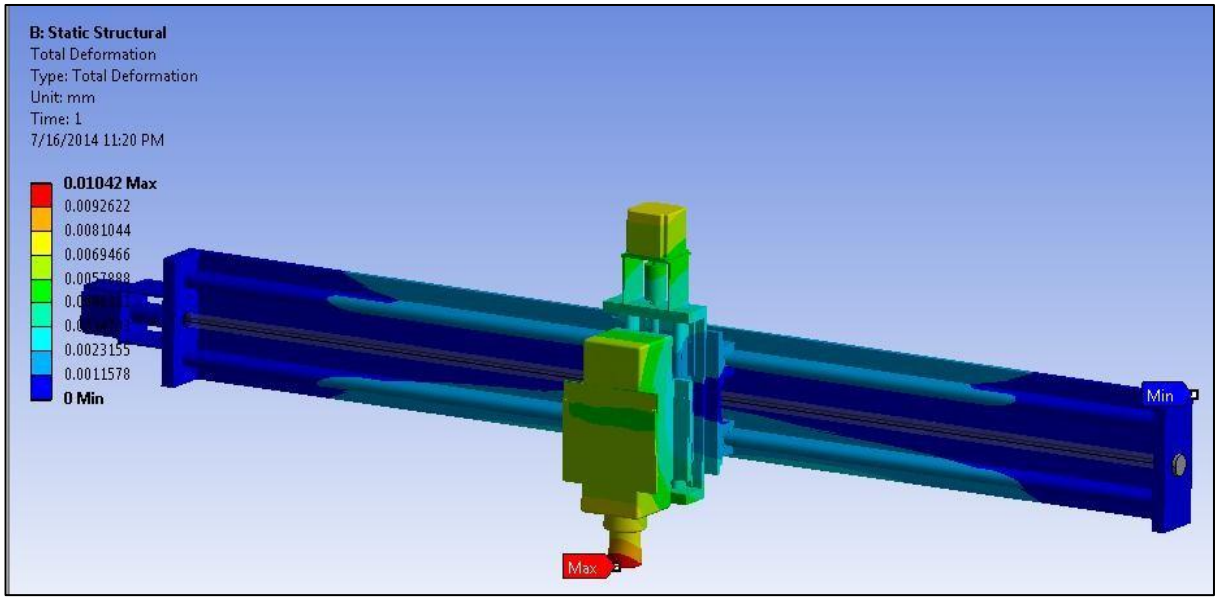

Figure 4.24: Maximum deflection in Y-axis Drive with 25.4 mm shaft

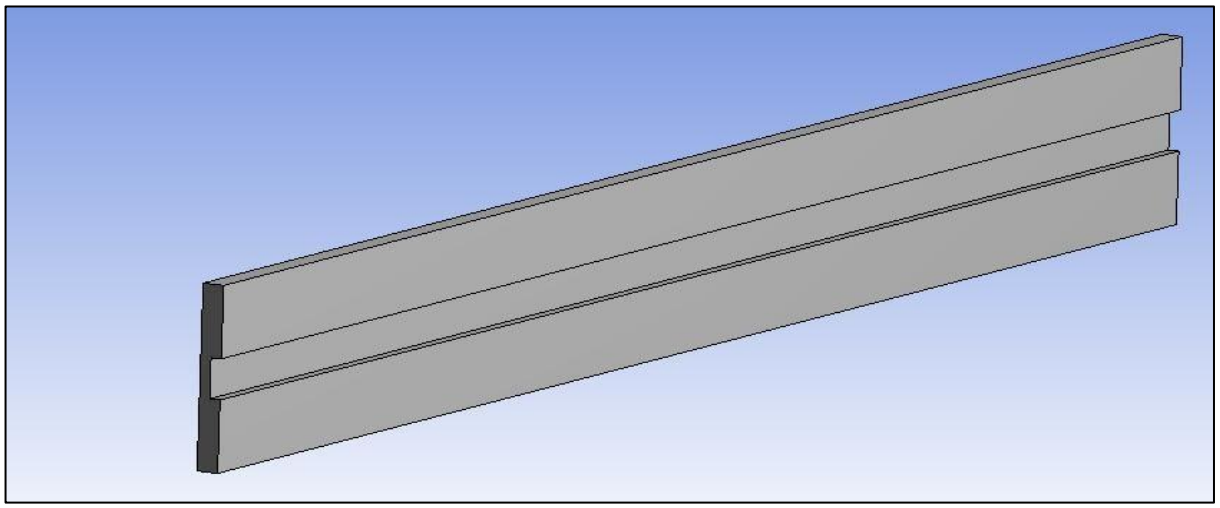

Figure 4.25: Aluminum back plate profile

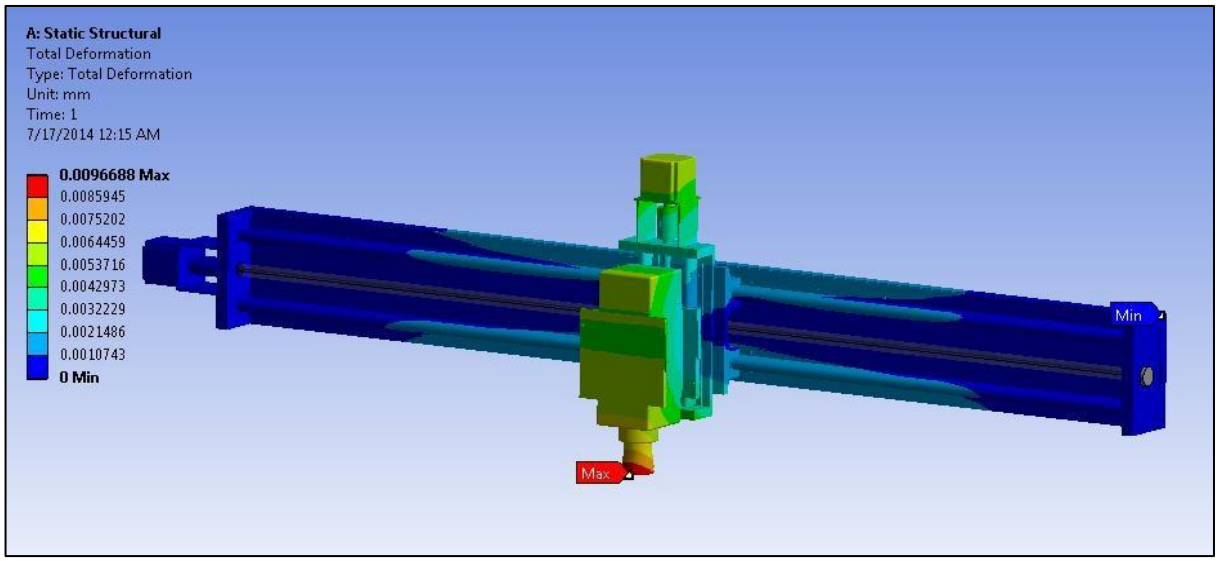

Figure 4.26: Maximum deflection in Y-axis Drive with aluminum back plate attached

4.8 SIDE PLATE

The side plate which will assemble the Y-axis drive with the X-axis drive cannot in general find out by numerical methods but its height is and can be varied according to the Z-axis traverse required .iteration on different shapes of the side plate was carried out in ANSYS . The deformation with simple flat plate was done with thickness 25 mm but the deformation was not going below 85 micron as shown in figure 4.28. The taper side plate was then chosen which considerably reduce the value to near 55 micron as shown in figure 4.29. It was seen that by broadening the plate at top by 100 mm the deflection was reaching nearly to 50 micron as shown in figure 4.30.The material of the all components were same and structural steel was used for the side plates.

Table 4.30: Material of components for analysis of Y-axis

Component	**Material**
Bracket plate	Aluminum 6061O
Bolt	Stainless steel
Back plate	Structural steel
Spindle	Structural steel
Coupling	Polyurethane
Ball screw of Z-axis and Y-axis	Chrome steel
Round shaft of Z-axis and Y-axis	Stainless steel
Supporting rail of shaft of Z-axis and Y-axis	Aluminum 6061O
Slide base plate of Z-axis and Y-axis	Structural steel
Side plate	Structural steel

The boundary condition were applying fixed support to the base of the side plate shown by symbol B, standard earth gravity was given to consider the self weight of the system and a remote force was applied shown in figure 4.27

Table 4.31: Iteration value for different shape of side plate

Simple flat side plate of thickness 25 mm		
Direction of Force	**Deflection**	**Von-mises Stress**
Positive X	0.08788 mm	9.0585 Mpa
Negative X	0.05596 mm	5.6098 Mpa
Positive Y	0.04857 mm	5.8400 Mpa
Negative Y	0.04341 mm	5.7280 Mpa
Z-direction	0.03447 mm	3.6937 Mpa
Taper plate with rib		
Direction of Force	**Deflection**	**Von-mises Stress**
Positive X	0.05561 mm	9.1076 Mpa

Negative X	0.03748 mm	4.1901 Mpa
Positive Y	0.03336 mm	5.7489 Mpa
Negative Y	0.03218 mm	5.6082 Mpa
Z-direction	0.02248 mm	3.0502 Mpa
Taper plate with rib and width 100 mm at top		
Direction of Force	**Deflection**	**Von-mises Stress**
Positive X	0.05126 mm	9.0558 Mpa
Negative X	0.03506 mm	3.9971 Mpa
Positive Y	0.03048 mm	5.6810 Mpa
Negative Y	0.03047 mm	5.4780 Mpa
Z-direction	0.02017 mm	3.0002 Mpa

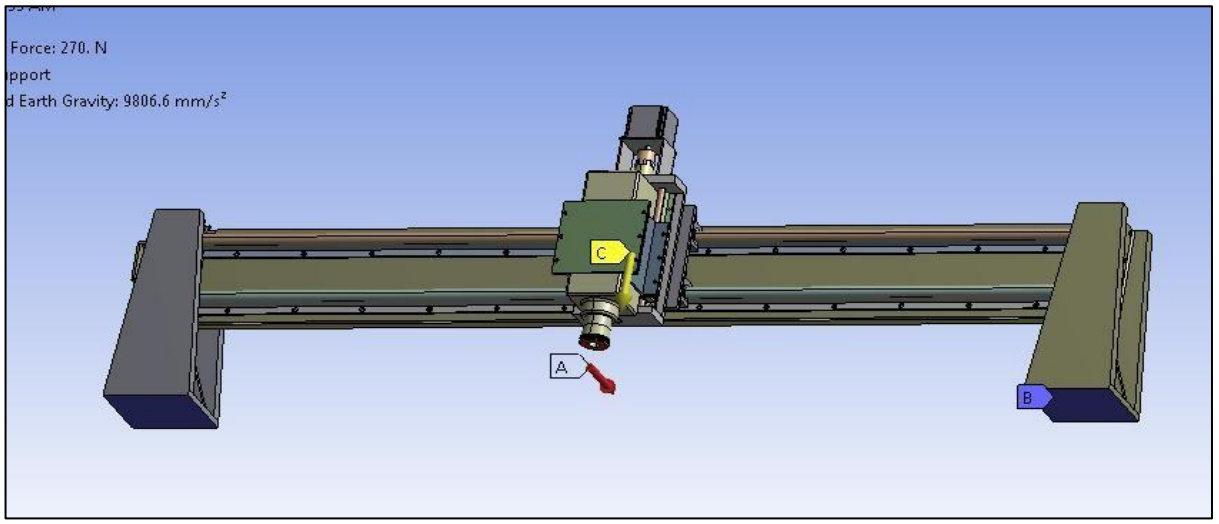

Figure 4.28: Boundary condition for side plate analysis

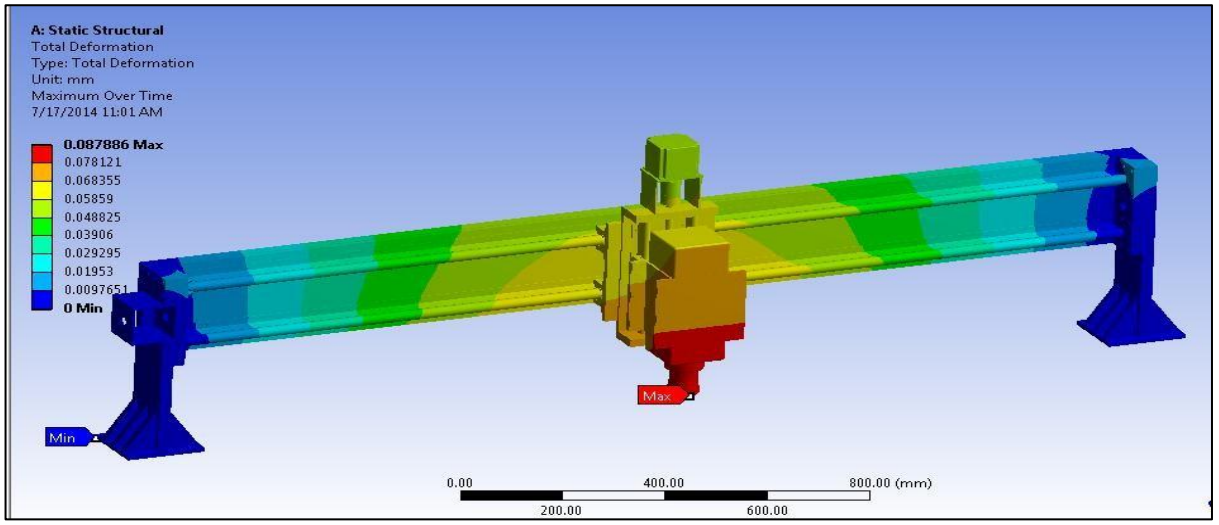

Figure 4.28: Flat side plate

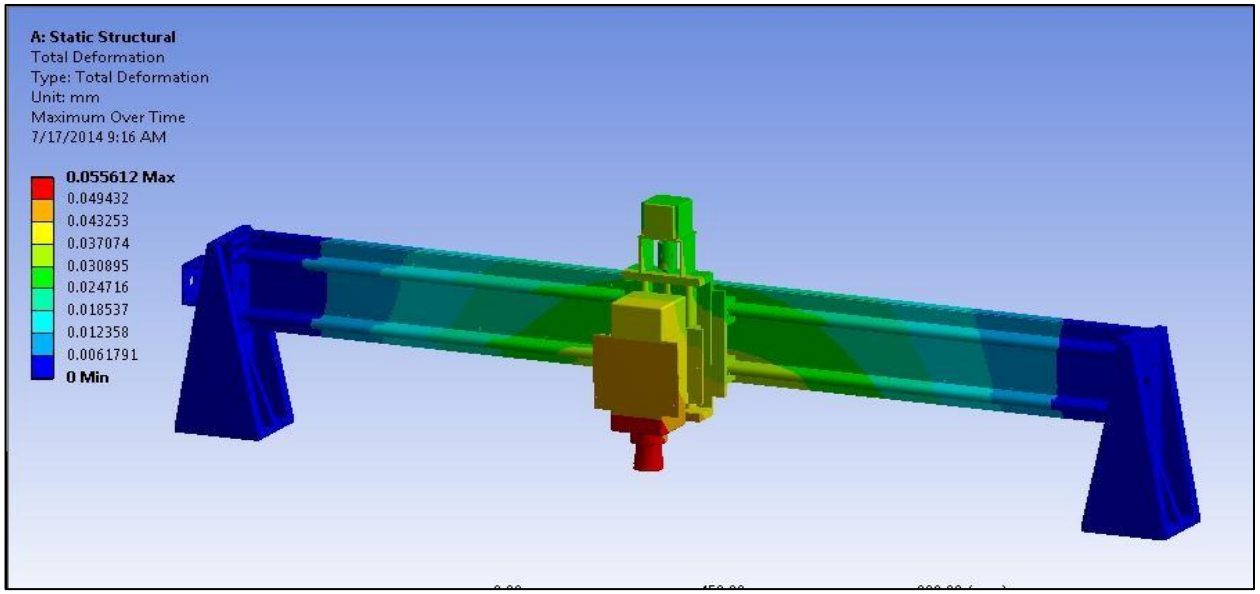

Figure 4.29: Taper plate

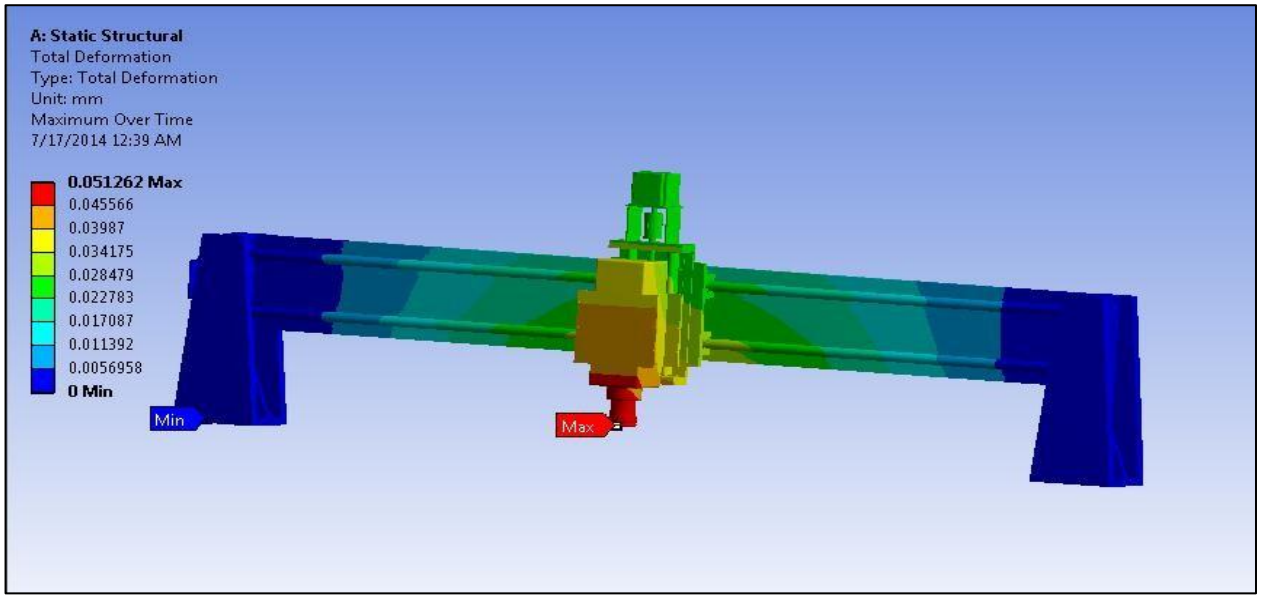

Figure 4.30: Taper plate with broad at top

4.9. X-AXIS DRIVE SELECTION

The selection of X-axis traverse were as similar as that of Y-axis and Z-axis drive except the selection of slide way. The slide way is not under any bending moment in case of X-axis and is only under direct compressive load in which the material shows very good strength. Therefore the design of X-axis was not in the scope of the present work but can be done in future by the reference of the present work.

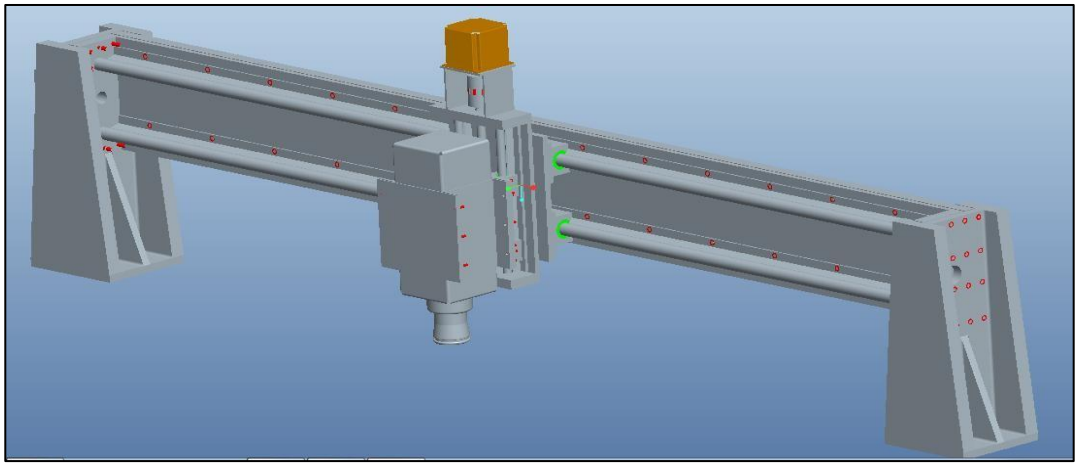

Figure 4.31: Final CAD model of the Design

4.10 CONCLUSION OF RESULTS AND DISCUSSION

The design process followed to minimize the deflection was found to be effective as the deflection in most of the members were under 10 micron and the overall deflection in the system was reduced to 50 micron. The maximum deflection was in the tool and the spindle due to cumulative addition of the various components deflection. So by proper designing method it can be further reduced by the study and selection of each component separately. Mainly the dimension of the non standard components were find out in this chapter by analysis namely bracket, back plate of Y-axis and the Side plate, where as the selection of standard components were verified.

CHAPTER 5

CONCLUSION AND FUTURE SCOPE

5.1. CONCLUSION OF THE PRESENT WORK

The FEM analysis of the machine tool drives in chapter 4 justify the components selected through design process and optimization is done if the deflection value exceeds the allowable value. As far as possible selection of standard components are preferred for the ease of machine tool construction while the non standard components such as Bracket are designed simple to manufactured.

The following conclusion can be made from the work:

(i) Bracket designed is safe to hold the spindle and thickness is optimized.

(ii) The Z-axis drive deflection is below 5 micron and Y-axis drive is below 10 micron instead of having a long drive distance of 2032 mm.

(iii) The different shape of the side plate of joining Y-axis and X-axis is iterated and result was found satisfactory with tapered plate whose result can be further improved by increasing the width of plate.

(iv) The round shaft selected has large range of models according to the cutting forces and supports the load satisfactorily within the safe limits.

(v) The cutting feed of 1.5 m/min with tool diameter of 1 inch was designed safely

5.2. Future Scope of the work

The work done here was focused toward setting up the empirical relation to various machine components and finding out the design procedure. Its study has been done thoroughly and interdependency is finding out which affects each other. The Analysis part done in the ANSYS was to validate these results and moving towards the optimization but there is huge scope for the future work as follow:

(i) Optimization of the machine tool structure with improved structure design can be done.

(ii) Dynamic analysis of the structure.

(iii) Considering the thermal and preload effects in ball screw to improve the results.

(iv) Cost analysis of the structure.

REFERENCES

[1] Stefan Holmberga, Kent Perssona, Hans Peterssonb, Nonlinear mechanical behaviour and analysis of wood and fiber materials, Computers & Structures Volume 72, Issues 4–5, August–September 1999, Pages 459–480

[2] J.kopac and S.Sali, Wood:an important material in manufacturing technology,journal material processing Technology,volume 133,issue 1-2,feb 2003,pages 134-142

[3] A. Malkoc-ogˇ lu, Machining properties and surface roughness of various wood s pecies planed in different conditions, Building and Environment, Volume 42, Issue 7, July 2007, Pages 2562–2567

[4] S. Rawangwong, J. Chatthong, J. Rodjananugoon, The Study of Proper Conditions in Face Coconut Wood by CNC Milling Machine, Quality and Reliability (ICQR), 2011 IEEE International Conference on 14-17 Sept. 2011 Page(s): 455 - 459

[5] J´er´emie Boucher, Pierre-Jean M´eausoone, Patrick Martin, S´ebastien Auchet and Lionel Perrin ,Influence of helix angle and density variation on the cutting force in wood-based products machining, Journal of Materials Processing Technology, Volume 189, Issues 1–3, 6 July 2007, Pages 211–218

[6] Maria Stefania Carmeli,Francesco Castelli Dezza , Marco Mauri, Luigi Piegari Energy Recovery and efficiency optimization in a wood cutting machines, Clean Electrical Power (ICCEP), 2013 International Conference on Year: 2013 , Page(s): 524 - 528

[7] Mohsen Soori, Behrooz Arezoo∗, Mohsen Habibi, Virtual machining considering dimensional, geometrical and tool deflection errors in three-axis CNC milling machines, Journal of Manufacturing Systems,2014

[8] M.Y yang and J.G. chui, A tool deflection compensation system for end milling accuracy improvement, Journal of Manufacturing Science and Engineering | Volume 120 | Issue 2,2008

[9] M. F. Zaehl, Th. Oertlil, Finite Element Modelling of Ball Screw Feed Drive Systems, CIRP Annals - Manufacturing Technology Volume 53, Issue 1, 2004, Pages 289–292

[10] Jerzy Z. Sobolewski Vibration of the ball screw drive. Engineering Failure Analysis

Volume 24, September 2012, Pages 1–8

[11] Daisuke Kono, Takahiro Inagaki, Atsushi Matsubara, Iwao Yamajin ,Stiffness model of machine tool supports using contact stiffness, Precision Engineering Volume 37, Issue 3, July 2013, Pages 650–657

[12] B. Li, J. Hong, Z. Wang, W. Wu and Y. Chen, Optimal Design of Machine Tool Bed by Load Bearing Topology Identification with Weight Distribution Criterion. ProcediaCIR,Volume3, 2012, Pages 626–631 45th CIRP Conference on Manufacturing Systems 2012

[13] M. F. Zaehl, Th. Oertlil and J. Milberg Finite Element Modeling of Ball Screw Feed Drive Systems. CIRP Annals - Manufacturing Technology Volume 53, Issue 1, 2004, Pages 289–292

[14] Anders Jo¨nsson, Johan Wall and Go¨ran Broman, "A virtual machine concept for realtime simulation of machine tool dynamics", International Journal of Machine Tools & Manufacture, vol. 45, pp. 795–801, 2005.

[15] Tomoya Fujita, AtsushiMatsubara, KazuoYamazaki, Experimental characterization of disturbance force in a linear drive system with high-precision rolling guideways, International Journal of Machine Tools and Manufacture Volume 51, Issue 2, February 2011, Pages 104–111

[16] Paweł Majda. Modeling of geometric errors of linear guide way and their influence on joint kinematic error in machine tools. Precision Engineering, Volume 36, Issue 3, July 2012, Pages 369–378

[17] Y. Altintas , A. Verl , C. Brecher , L. Uriarte and G. Pritschow Machine tool feed drives, CIRP Annals - Manufacturing TechnologyVolume 60, Issue 2, 2011, Pages 779–796

[18] Y.altintas, A.verl, C.Brecher, L.Uriate,G.Pritshow, Machine tool feed drives,CIRF Manufacturing technology, volume60, issue 30,2011,pages 779-796

[19] Janez Gradisˇek , Martin Kalveram , Klaus Weinert Mechanistic identification of specific force coefficients for a general end mill. International Journal of Machine Tools and Manufacture Volume 44, Issue 4, March 2004, Pages 401–414

[20] S. Doruk Merdol, Yusuf Altintas , Virtual cutting and optimization of three-axis milling processes, International Journal of Machine Tools and Manufacture Volume 48, Issue 10, August 2008, Pages 1063–1071

[21] Shaolua HU,Fei Liu,Yan He and Bin Peng, Charctertics of addition loss in spindle system of machine tool,Journal of advance machine design system and manufacturing.Aug 2010

WEB REFERENCES

[22] http://en.wikipedia.org/wiki/Wooden_spoon

(Downloaded on March 20, 2014)

[23] http://en.wikipedia.org/wiki/Samuel_Bentham
(Downloaded on May 16, 2014)

[24] http://www.aliexpress.com/item-img/3-axis-mini-cnc-router/657864064.html
(Downloaded on May 16, 2014)

[25] (Downloaded on Dec 02, 2013)

[26] www.ebay.com/itm/CAD-CAM-3D-CNC-router-milling-software-toolpath-Meshcam-Art-Sherline-Mach-3-/251011588280
(Downloaded on May 16, 2014)

[27] http://www.actioncnc.com/Roland_MDX-40_Desktop_CNC_Mill.htm
(Downloaded on June 12,2014)

[28] http://www.5axiscncrouter.com/5axisCNCrouterwithmovingbridge.html

(Downloaded on June 12,2014)

[29] http://www.technocnc.com/technical-section/before-purchasing-cnc-router.htm

(downloaded on june 11,2014)

[30] http://www.hiwin.com/

[31] http://www.pbclinear.com/

[32] www.samstores.com/Store.asp?intPageSizea=25&sort=5&PageNo=34&PrNew=1
(Downloaded on may 17,2014)

[33] http://www.craftmachinetools.co.za/Products/Feeder.aspx

(Downloaded on may 17,2014)

[34] http://0531sudiao.en.busytrade.com/products/info/1893737/Wood-Cnc-Engraving-Machine-With-Vacuum-Hold-Down.html

(Downloaded on may 17,2014)

[35] Akhil mahajan, fabrication and design evaluation using cae tools for a 3-axis vertical milling machine for sculptured surface machining,ME thesis, Thapar University, july 2012

[36] V.B. Bhandari , " Design of machine Elements" Tata McGraw-Hill Education, 2010

[37] http://www.learneasy.info/MDME/MEMmods/class_projects/backstop/controller/Topic4-BallscrewCalculations.pdf

(Downloaded on NOV,2013)

[38] www.ktr.com

[39] matweb.com/search/PropertySearch.aspx

[40] http://www.thk.com/